Biological Potential of Carbazole Derivatives

ARTICLE *in* EUROPEAN JOURNAL OF MEDICINAL CHEMISTRY · MARCH 2015

Impact Factor: 3.45 · DOI: 10.1016/j.ejmech.2015.02.059 · Source: PubMed

1 AUTHOR:

Agata Głuszyńska
Adam Mickiewicz University
18 PUBLICATIONS **209** CITATIONS

SEE PROFILE

European Journal of Medicinal Chemistry 94 (2015) 405–426

Contents lists available at ScienceDirect

European Journal of Medicinal Chemistry

journal homepage: http://www.elsevier.com/locate/ejmech

Invited review

Biological potential of carbazole derivatives

Agata Głuszyńska

Laboratory of Bioanalytical Chemistry, Faculty of Chemistry, A. Mickiewicz University, Umultowska 89b, 61-614 Poznań, Poland

ARTICLE INFO

Article history:
Received 30 August 2014
Received in revised form
19 February 2015
Accepted 28 February 2015
Available online 3 March 2015

Keywords:
Carbazole derivatives
Biological potential
Antimicrobial activity
Neurological disorders
Antitumor activity
DNA

ABSTRACT

Carbazole skeleton is the key structural motif of many biologically active compounds including synthetic and natural products. Over the past several years, a large number of research highlighting the significance of carbazole derivatives has been reported in the literature. The present review focuses on the recent progress, from 2010 until now, in knowledge on various biological properties of classical, tricyclic carbazole derivatives.

1. Introduction

Carbazole is a tricyclic compound with the carbon skeleton of fluorene, occurring in coal tar. Due to its fluorescent properties, carbazole ring system is a structural element of many compounds used in electronics for the production of electroluminescent materials [1–4], polymers [5–9] or dyes [10,11]. Very interesting biological properties of active carbazole alkaloids, isolated mainly from taxonomically similar plants of the genus *Murraya*, *Glycosmis* and *Clausena* in the family *Rutaceae* caused that many research groups became interested in the structural modifications of natural compounds and synthesis of new derivatives of carbazole [12]. There are known biologically active fused aromatic systems of natural origin (alkaloids) or synthetic drugs containing in their structure an element of carbazole [12–27] as well as derivatives of tricyclic carbazole [12,23–32], which possess anti-cancer, antibacterial, antifungal, anti-inflammatory, hepatoprotective, anti-HIV, anti-protozoan and sedative properties, or topoisomerase II inhibition ability.

In this article I will present only the derivatives of classical, tricyclic carbazole reported within the last 10 years, which are interesting because of their biological and photophysical properties [33–89]. Some of carbazole compounds have a very high activity against many organisms: bacteria, fungi, parasites [33–37], or are potential anti-inflammatory agents [38]. Some derivatives of carbazole are potential multifunctional agents for the treatment of neurological disorders [39–52], others show strong or moderate antitumor activity against different cell lines by a variety of mechanisms [53–72]. Small organic compounds can non-covalently interact with DNA through intercalation, the minor groove binding or electrostatic interactions. Most classical ligands interact with double-stranded DNA, which often is the object for testing the activity of new drugs and compounds of potential biological importance. Recently, the DNA binding studies have been extended into selective ligands capable of intercalation to the triple stranded DNA helix (triplex) and stabilization of the guanine tetraplex DNA (G-quadruplexes, G4 DNA). The latter unique structures may involve one- or more strands of nucleic acids and was first described by Gellert et al. [90]. The first report about biological activity of G4 DNA (inhibition of human telomerase) was published by Sun et al., in 1997 [91]. Since that time there have been numerous reports in the literature on the various “G-quadruplex” ligands with potential anti-cancer properties [92–97]. Family of ligands able to interact with different forms of nucleic acids also includes carbazole derivatives [73–88]. Among them, one derivative, 3,6-bis[2-(1-methylpyridinium)vinyl]carbazole (BMVC), can be recognize as specific for quadruplex structures, particularly towards the quadruplex of human telomeric sequence $d(T_2AG_3)_4$. Moreover, it showed remarkable inhibition of telomerase ($IC_{50} = 0.05\ \mu M$) [82–87] Table 1.

E-mail address: aglusz@amu.edu.pl.

http://dx.doi.org/10.1016/j.ejmech.2015.02.059
0223-5234/

Table 1
Biological activity of carbazole derivatives.

2.1. Antimicrobial activity

Target/species		Tested compounds	Reference
Bacterial species	*Proteus mirabilis*	**1a–f**	[33]
	Proteus vulgaris	**1a–f**	[33]
	Proteus spp.	**2a–c**, **3a–c**, **4a–c**, **5a–c**, **6**, **7**	[34,35]
	Pseudomonas aeruginosa	**2a–c**, **3a–c**, **4a–c**, **5a–c**, **6**, **7**	[34,35]
	Pseudomonas spp.	**7**	[35]
	Bacillus subtilis	**2a–c**, **3a–c**, **4a–c**, **5a–c**, **6**	[34]
	Salmonella typhi	**1a–f**	[33]
	Escherichia coli	**2a–c**, **3a–c**, **4a–c**, **5a–c**, **6**, **7**	[34,35]
	Klebsiella pneumonia	**7**	[35]
	Staphylococcus aureus	**1a–f**, **2a–c**, **3a–c**, **4a–c**, **5a–c**, **6**	[33,34]
Fungal species	*Rhizoctonia solani*	**1a–f**	[33]
	Macrophomina phaseolina	**1a–f**	[33]
	Curvularia lunata	**1a–f**	[33]
	Alternaria alternata	**1a–f**	[33]
	Candida albicans	**2a–c**, **3a–c**, **4a–c**, **5a–c**, **6**, **7**	[34,35]
	Aspergillus fumigatus	**2a–c**, **3a–c**, **4a–c**, **5a–c**, **6**,**7**	[34,35]
	Aspergillus niger	**7**	[35]
	Aspergillus flavus	**7**	[35]
	Penicillium species	**7**	[35]
Yeast	*Saccharomyces cerevisiae*	**8a**,**b**, **9a**,**b**, **10**, **11**, **12**, **13**, **14**, **15**, **16**	[36]
Parasites	*Plasmodium* species, e.g. *P. falciparum* K1	**19a–h**, **18**, **8c**,**d**	[37]

2.2. Neurological disorders

Target/activity		Tested compounds	Reference
K562 and GLC4 cell lines	Inhibition of formation of Beta-amyloid (Aβ) peptides	**21a**	[41]
Human neuroblastoma SH-SY5Y neuronal cells	Inhibition of aggregation of Beta-amyloid (Aβ) peptides	**22a–d**	[40]
γ -Secretase	Inhibition of formation of Beta-amyloid (Aβ) peptides	**23b**	[39]
Neuroblastoma NG 108-15 cells, glial cells C6	Cholinesterase inhibition; anti-oxidant activity; neuroprotective activity	**26a–c**	[42]
Neurons	Hippocampal neurogenesis	**19i**,**j**,**k**,**l**, **27–32**	[43,44]
Neural stem cells	Neurogenesis	**19i**,**j**,**k**,**m**	[45]
Neuroblastoma N1E-115 cells	Neuroprotective activity	**33**	[48]
AD mouse models TgCRND8 and Tg2576; Wistar rats	Anti Aβ-fibrylation/oligomerization activity; neuroprotective activity; anti-oxidant activity	**33**	[46,47,50]
Mice hippocampal HT22 cells	Nrf2/ARE; anti-oxidant activity;	**33**, **34a–e**	[49,51]
Murine microglia cell line N9	Anti-oxidant activity	**35**	[52]

2.3. Antitumor activity

Target/Cell lines		Tested compounds	Reference
Leukemia	THP-1 monocytic	**35**	[53]
	CEM (T-cell)	**35**, **37**	[53,54]
	Molt-3 (T-cell)	**37**	[54]
	HL60	**35**, **40c**,**d**,**e**	53,57
Prostate	DU145	**37**	[54]
	PC3	**35**, **37**, **40c**	[53,54,57]
Lung	DMS79	**37**	[54]
	A549	**38**	[55]
	H1299	**41a**, **42**	[60,61,65,68]
	CL1-0	**41a–j**, **43**	[62,65,67–69,71]
	TC-1	**41a**	[66]
	CL1	**41a**	[60]
	MRC-5 (fibroblast)	**40c**, **41a–j**	[57,60,62,68,69,71]
	IMR90 (fibroblast)	**41a**	[60,61]
Cervix	HeLa	**41a**, **42**	[60,61,65,67]
Melanoma	DND-1	**37**	[54]
Hepatoma	Bel-7402	**37**	[54]
Breast	MCF7	**21a**,**b**, **35**, **37**, **38**, **39**, **40c**, **41a–j**, **42**	[53–57,62,65,67,81]
	Hs578T	**39**	[56]
	MDA-MB-231	**21a**,**b**	[81]
Colon	HT29	**35**	[53]
	HCT116	**40c**	[57]
Neuroblastoma	SK-N-SH	**38**	[55]
Nasopharyngeal	KB	**40**	[57]
	KJ-1	**41a**	[60,84]
Oral cavity	Ca9-22	**41a**	[60]
Skin (fibroblast)	Detroit-551	**41a**	[60]
	Keratinocyte HaCaT	**41a**	[60]
	BJ	**41a**	[62]
	BJ1	**41a**	[60,61]
Mouse fibroblast	NIH3T3 embryonic	**41a**	[68]
	BALB/c 3T3, clone A31-1-1	**41a**	[70]

Table 1 (*continued*)

2.4. Interaction with DNA			
Target/Sequence (5' → 3')		Tested compounds	Reference
G4 DNA	T_2AG_3 (Hum6)	**41m,n**	[88]
	$(T_2AG_3)_2$ (Hum12)	**41a**	[82,85]
	$(T_2AG_3)_4$ (HT24,H24)	**41a**, **42**, **43**	[59,63,65,67,82–85,87]
	$GGG(T_2AG_3)_3$ (H21)	**41a**	[85,87]
	$AG_3(T_2AG_3)_3$ (HT22)	**21a,b**, **41k,l,m,n**, **45a,b**, **47**	[73,75,78,79,85–88]
	$TAG_3(T_2AG_3)_3$ (HT23)	**41a,j**, **43**	[65,67]
	$TAG_3(T_2AG_3)_3TT$ (HT25)	**41a**, **43**	[65]
	$(T_2AG_3)_4TT$ (H26)	**41a**	[85,87]
	$AG_3(T_2AG_3)_7$ (HT46)	**21a**, **b**	[79]
	$(TTAGGG)_9$ (H54)	**41a**	[85,87]
	$(TTAGGG)_{13}$ (H78)	**41a**	[85,87]
	$T_2AG_3T_3G_3(T_2AG_3)_2$ (H24-T9)	**41a**	[85,87]
	$(T_2AG_3)_2T_3G_3T_2AG_3$ (H24-T15)	**41a**	[85,87]
	$(T_2AG_3)_2T_2G_3T_2AG_3$ (M23)	**41a**	[85,87]
	$(T_2AG_3)_2T_4G_3T_2AG_3$ (M25)	**41a**	[85,87]
	AGGG $(T_2AG_3)_3TT$ (H24-B)	**41a**	[85]
	$(G_3T_2A)_3G_3T$ (HT21-T)	**41a**, **43**	[65,67]
	$TGAG_3TG_3TAG_3TG_3TAA$ (c-myc)	**41k,l**, **47**	[75]
	$G_3CG_3CGCGAG_3AG_4$ (c-kit2)	**41k,l**, **47**	[75]
	$G_4T_4G_4$ (Oxy12)	**41a**	[82]
	$(T_2G_4)_2$ (Tet12)	**41a**	[82]
	$G_2T_2G_2TGTG_2T_2G_2$ (Apt)	**41a**	[82]
	$G_4(T_4G_4)_3$ (Oxy28)	**41a**	[82]
	TG_4T (LQ1)	**41a**	[82]
	T_4G_4 (LQ4)	**41a**	[82]
	$G_2T_2G_2TGTG_2T_2G_2$ (TBA)	**41a**, **43**	[65,67]
	$TGAG_3TG_4AG_3TG_4AA$ (PU22)	**41a**, **43**	[65,67]
	$(TAG_3)_2TG_3TAG_3$ (GT19)	**41a**, **43**	[65]
	$G_3(TG_3)_3$ (T3)	**41a**, **43**	[65]
	$(G_3C)_4$ (T40214)	**41a**, **43**	[65,67]
	$G_2TG_2TG_2TG_2TTGTG_2TG_2TG_2TG_2$ (AS1411)	**41a**	[67]
	TGAGTGTGTTGAGTGTGTTGAA (PU22M)	**41a**	[67]
	$G_5CCACCG_3CAG_5CG_5$ (WNT1)	**41a**, **42**	[72]
Double-stranded DNA	ctDNA	**7**, **21a–c**, **40a–e**, **41a**, **43**, **45a–d**, **46**, **48**	[35,57,65,73,74,78,79,80,82]
	$[d(GCGCAATTGCGC)]_2$ (LD12)	**41a**, **43**	[65,82]
	$[d(ATGCGCA_2T_2GCGCAT)]_2$ (LD)	**41a**	[83,84]
	$Poly[dA\text{-}dT]_2$	**21c**, **45a–d**, **48**	[73,80]
	$Poly[dG\text{-}dC]_2$	**21a–c**, **45a–d**, **48**	[73,79,80]
	Poly[dA] * Poly[dT]	**21a–c**, **48**	[79,80]
	Poly[dG] * Poly[dC]	**21c**, **48**	[80]
	$(AT)_6$ (AT)	**41a**	[82]
	$(GC)_6$ (GC)	**41a**	[82]
	$d(CGAATTCG)_2$	**45a,b**	[73]
	CGCGAAATTTCG-CG (drewAT)	**41k,l**, **47**	[75]
	CAATCGGATCGAATTCGATCCGATTG (ds26)	**41k,l**, **47**	[75]

2. Biological activities of carbazoles

2.1. Antimicrobial activity

Carbazole ring is present in various natural medicinal active substances [12–32]. More recently macrocyclic diamides based on carbazole skeleton with thia- and oxy-linkage systems have been synthesized. Six new compounds **1a–f** with the structural elements of biological importance showed significant antibacterial and antifungal activity (Fig. 1) [33].

Antimicrobial activities of compounds were tested against four human pathogenic bacteria such as *Proteus mirabilis*, *Proteus*

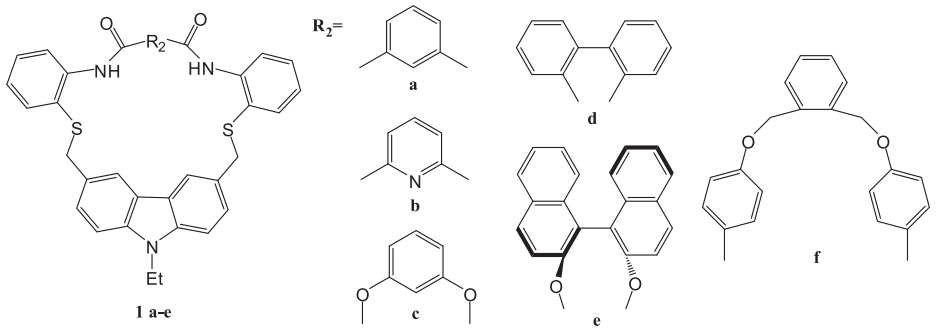

Fig. 1. Structures of carbazolophanes **1a–f**.

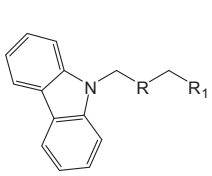

2-5 a,b,c

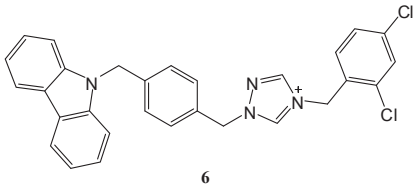

6

Compound	R	R_1
2a	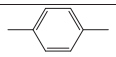	
2b	$-(CH_2)_2-$	
2c	$-(CH_2)_4-$	
3a	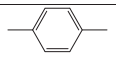	
3b	$-(CH_2)_2-$	
3c	$-(CH_2)_4-$	
4a	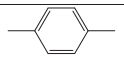	
4b	$-(CH_2)_2-$	
4c	$-(CH_2)_4-$	
5a	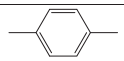	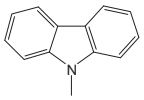
5b	$-(CH_2)_2-$	
5c	$-(CH_2)_4-$	

Fig. 2. Structures and the structural elements of the N-substituted carbazole derivatives **2**–**6**.

vulgaris, *Staphylococcus aureus* and *Salmonella typhi*. Antifungal activity of these compounds was also tested against four plant pathogenic fungi such as *Rhizoctonia solani*, *Macrophomina phaseolina*, *Curvularia lunataand*, *Alternaria alternata*. The screening of amides **1a**–**f** for their biological activity expressed by minimum inhibitory concentration (MIC), was performed *in vitro* conditions with the use of a control sample (10% DMSO) and commercial antibiotics, tetracycline (for human pathogenic bacteria) and carbendazim (for plant pathogenic fungi). The antibacterial (MIC_{50} = 5–80 μg/ml) and antifungal (MIC_{50} = 10–45 μg/ml) activity of the tested compounds were dose dependent and were remarkable at higher concentrations. The carbazolophanes **1b** and **1e** exhibited good antibacterial and antifungal activities against all pathogens. Compound **1e** with element of (*S*)-BINOL showed excellent antibacterial and antifungal activity, much better antibacterial activity on tested human pathogens than that for commercially available antibiotics, tetracycline and carbendazim.

Azole moieties such as imidazole and triazole are important

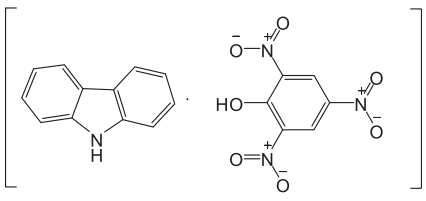

7

Fig. 3. Structure of carbazole picric acid (CP) adduct **7**.

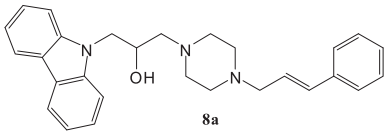

8a

Fig. 4. Structure of Incentrom A **8a**.

pharmacophores occurring widely in various types of pharmaceuticals that possess a variety of pharmacological activities. Therefore, Zhou and cooperators received a series of N-substituted carbazole derivatives **2**–**6** with the imidazole (**3a**–**c**) and triazole (**4a**–**c**, **6**) moieties, and tested their antibacterial and antifungal properties (Fig. 2) [34].

These novel derivatives of carbazole, besides of possessing different azole moieties, varied in the length of linker R substituted to the nitrogen atom (4 or 6 carbon atoms) and in the electronic nature of linker (an aromatic ring against aliphatic chain) (Fig. 2). *In vitro* studies were carried out against strains of *S. aureus*, methicillin-resistant *S. aureus* (MRSA), *Bacillus subtilis*, *Escherichia coli*, *Pseudomonas aeruginosa*, *Bacillus proteus*, *Candida albicans* and *Aspergillus fumigatus*. The best antibacterial activity (MIC_{50} = 1–8 μg/ml) showed compounds **3a**–**c** with imidazole substituent. Replacement of the imidazole substituent with triazole one (**4a**–**c**) resulted in a reduction of antibacterial activity (MIC_{50} = 16–512 μg/ml), whereas the antifungal activity against *C. albicans* increased. The introduction of the charge in order to increase the aqueous solubility and to increase the biological activity returned intended effect – compound **6** showed a very good fungicidal activity (MIC_{50} = 2–8 μg/ml) compared to unsubstituted analogs **4a** (MIC_{50} = 256–512 μg/ml). Some of the synthesized compounds showed comparable or even better antibacterial and antifungal properties against these strains than the reference drugs: fluconazole, norfloxacin and chloramphenicol.

The new Carbazole Picric acid adduct (CP) **7** was obtained in order to test activity of carbazole moiety in a compound that possessed acidic properties (picric acid and its derivatives) (Fig. 3) [35]. The adduct exhibited noticeable antibacterial and antifungal activities against five Gram-negative bacteria *Proteus* species (sp.), *E. coli*, *P. aeruginosa*, *Pseudomonas* sp., *Klebsiella pneumonia* and five fungal species *Aspergillus niger*, *Aspergillus flavus*, *A. fumigatus*, *C. albicans* and *Penicillium* sp., respectively.

The *in vitro* experiments were performed at the adduct concentration of 100 μg/mL, using DMSO as a control, tetracycline and nystatin as standard drugs for the comparison of antibacterial and antifungal results, respectively. In the case of *P. aeruginosa*, *E. coli*, *Pseudomonas* sp. and *A. flavus*, *A. fumigatus*, *Penicillium* sp. the adduct **7** possessed inhibitory activity very similar to that of the standards.

Incentrom A **8a** is a compound that could be useful in diagnosis of yeast-specific growth inhibitors providing opportunities to develop novel antifungal drugs (Fig. 4). The mechanism of action is based on the process of chromosome segregation, which is done by specialized chromosomal structures called the centromeres (DNA region) and the kinetochore (protein assembly). The experimental model in such studies is yeast *Saccharomyces cerevisiae* that contains specific and absolutely essential DNA sequences for true

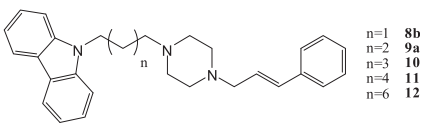

Fig. 5. Structure of Incentrom A derivatives **8b**, **9a**, **10**–**12**.

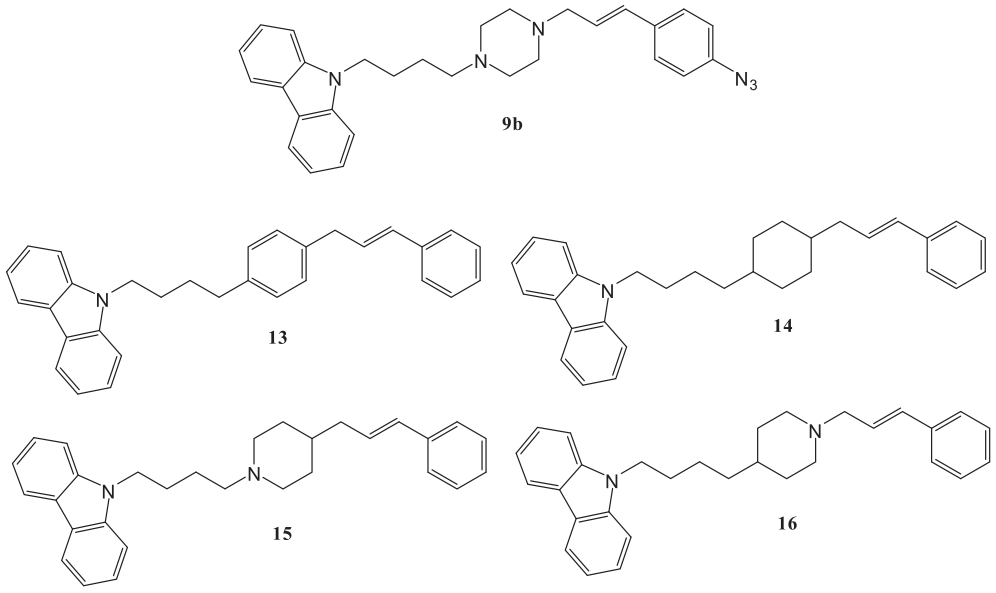

Fig. 6. Structures of Incentrom A derivatives **9b**, **13**–**16**.

chromosome segregation.

Lee et al. synthesized a series of Incentrom A analogs that inhibited the chromosome segregation process in yeast [36]. The minimum inhibitory concentration was established for each of the 48 new compounds. The structural elements of Incentrom A identified as pharmacophoric unit was piperazine ring substituted with two aromatic moieties through alkyl chains. The influence of different substituents, chain length between piperazine and carbazole, presence of two nitrogen atoms of piperazine, and importance of the carbazole ring on the drug activity were examined. The synthesis of enantiomerically pure analogs of Incentrom A **8a** (MIC = 15 μM) did not show any changes in activity (MIC = 14–16 μM). Introduction of a group bigger than hydroxyl (OBz, N_3) or the sp^2 center in the chain (C=O) resulted in a significant decrease in activity (MIC > 45 μM). Authors found, that removal of the hydroxyl group resulted in a significant increase of activity (MIC = 5–45 μM). Furthermore, the butyl and pentyl chains showed better activities (**9a**, **10** MIC = 5–6 μM) than other chain lengths (**8b**, **11**, **12** MIC = 7–45 μM). It turned out that the best activity has compound **9a** with 4-carbon chain between carbazole and piperazine rings without any substituent in the middle (Fig. 5).

The replacement of carbazole by indole or destruction of rigid carbazole ring resulted in loss of activity (MIC >45 μM). The results obtained with piperidine analogs of Incentrom A showed the importance of two nitrogen atoms in this moiety – the presence of nitrogen in the molecule was crucial (**13**, **14**, no activity), but the position of the nitrogen atom was not critical for the inhibitory activity (**15**, **16**, MIC = 4–13 μM) (Fig. 6). Introduction of an azide functional group to compound **9** resulted in the achievement of an inhibitor with excellent activity (**9b**, MIC = 5 μM, Fig. 6). Authors identified this compound as a photo-affinity probe suitable to isolate target proteins *in vivo*.

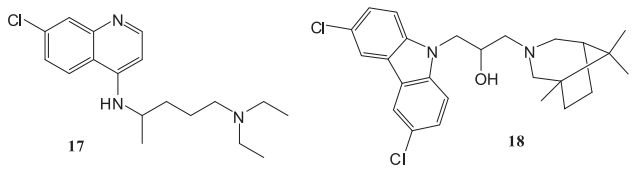

Fig. 7. Structures of chloroquine **17** and TDR30137 **18**.

One of the most dangerous parasitic diseases to this day remains malaria (about one million deaths per year) caused by parasites of the *Plasmodium* species. However, the *Plasmodium falciparum* strains are the most deadly. Some crude root extracts of the *Clausena harmandiana* show antiplasmodial activity against these strains due to presence of carbazole compounds [37]. As in the case of antibiotics, drug resistance of certain strains was observed also for well-known antimalarial drugs (e.g., chloroquine **17**, Fig. 7). Interestingly, naturally occurring compounds containing a carbazole unit as well as the synthetic carbazole derivatives exhibit antimalarial properties. Therefore, Tropical Diseases Research – the World Health Organization dependent institution, began collaboration with public and private sectors to screen several thousand compounds. Among them, the commercially available compound TDR30137 **18** related to N-substituted carbazoles showed excellent activity (IC_{50} = 57 nM) in *in vitro* screen against the chloroquine-resistant *P. falciparum* K1 (*Pf*-K1) in human red blood cells [37]. However, *in vivo* tests using the *Plasmodium berghei* mouse model compound didn't show any activity.

On the basis of structure of TDR30137 **18** substructure searches and the synthesis of new analogs were performed. The importance of carbazole, the aromatic moiety, the spacer, and the amine type were tested. The structure activity relationship (SAR) study permitted selection of compound with key potent feature as the substituted carbazole linked to an amine via a floppy chain. Many modifications led to inactive compounds, but 40 new analogs were refined.

The study has shown the importance of halogen substituents, the presence of a hydroxyl group (the ability to form hydrogen bonds) and basic character of amine for the activity of compounds on *P. falciparum*-K1 strains. The removal of one or two halogens from the carbazole moiety decreased the activity of compounds from IC_{50} = 9–16 nM to IC_{50} = 27–275 nM (respectively, **19f**,**g**,**h**, Fig. 8). The presence of the hydroxyl group is critical for the activity; no such group or its replacement by methoxy, carbonyl or fluoric substituents led to a significant loss in activity (respectively, **19d**,**h**,**c**,**b**, Fig. 8). At the same time the basic character of the amine moiety seems to affect the activity of the compounds, while the

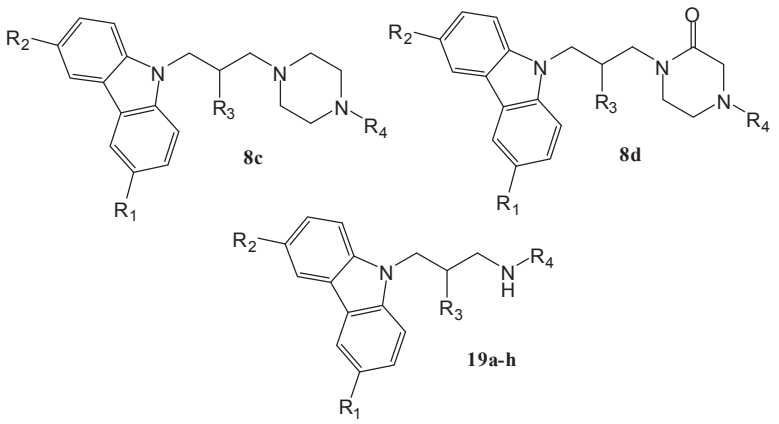

Compound	R_1	R_2	R_3	R_4	*Pf*-K1 IC_{50}[a]
19a	Cl	Cl	OH	CH_2-Cy	16 nM
19b	Br	Br	F		106 nM
19c	Cl	Cl	=O		448nM
19d	Cl	Cl	H		707 nM
19e	Br	Br	OH	Bn	27 nM
19f	Cl	H	OH		165nM
19g	H	H	OH		275 nM
19h	H	H	OCH_3		3313 nM
8c	Br	Br	OH	Cy	9 nM
8d	Cl	Cl	OH	Bn	344 nM

[a] A 72h assay in the presence of serum albumin

Fig. 8. Structures of aminoalcohol–carbazole derivatives.

introduction of a non-basic amide group reduced their activity (**8d**, Fig. 8). Since both compounds **8c** and **9a** showed very promising *in vitro* results, they were selected for *in vivo* study of activity using the *P. berghei* mouse model. Compound **8c** exhibited much better properties than its analog **19a**, and its enantiomers had the same activity against *Pf*-K1 as the racemate **8c**.

Following the trend of fusion research on the design and synthesis of biologically active small molecules Bandgar et al. have reported a new series of 15 compounds of 3-(substituted)-aryl-5-(9-methyl-3-carbazole)-1H-2-pyrazolines **20** (Fig. 9) [38]. All of them have been examined for their *in vitro* anti-inflammatory activity as well as their antioxidant activity.

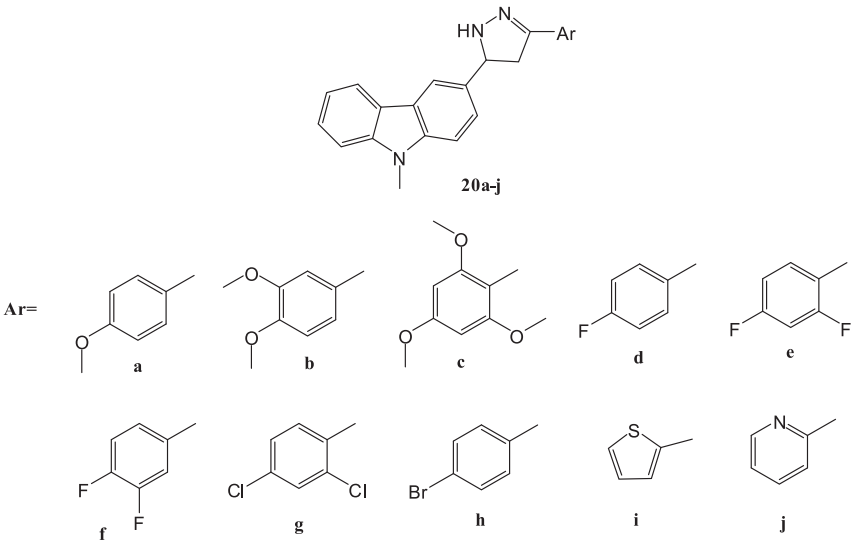

Fig. 9. Structures of 3-(substituted)-aryl-5-(9-methyl-3-carbazole)-1H-2-pyrazolines **20**.

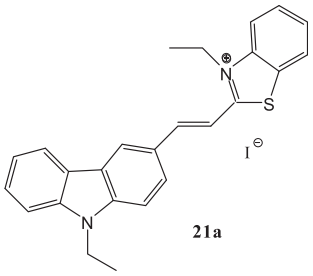

Fig. 10. Structure of carbazole thiazole (CT) **21a**.

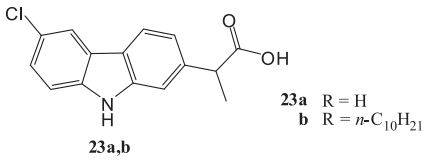

Fig. 12. Structure of carprofen **23a** and its N-decyl analog **23b**.

Compounds **20a**,**b**,**c** and **20i** showed potent COX-2 inhibition. Cyclooxygenase 2 (COX-2) is a form of cyclooxygenase (COX-1 and COX-2) and is induced in response to the release of a series of pro-inflammatory mediators. Its enzymatic activity would be of therapeutic value, because COX-2 is associated with inflammation and the resulting pain, and cancer proliferation. It has been established that many non-steroidal anti-inflammatory drugs (NSAIDs) interact with these enzymes and inhibit their enzymatic activity. However, the discovery of COX-2 selective inhibitors may increase the therapeutic power and reduce the classical side effects associated with the use of conventional NSAIDs. Compounds **20e**,**g** and **20j** have shown moderate inhibition of COX-2 but selectively inhibited enzyme COX-2, not a COX-1. Only compounds **20d**,**f** and **20h** were active against COX-1. Compound **20h** was an effective inhibitor of both COX-1 and COX-2. The COX-1, the second form of cyclooxygenase, is a constitutive enzyme responsible for the production of cytoprotective prostaglandins in the gastrointestinal tract (GI) and proaggregatory thromboxanes in blood platelets. The structure activity relationship (SAR) studies of the new compounds have shown the effect of the electron nature of substituents on the aromatic ring on COX-2 inhibition: electron donating groups cause increase of COX-2 inhibition, while the withdrawing groups its decrease (except for compound **20h**). The most active compounds **20a**,**b**,**c** and **20i** were evaluated for their *in vivo* inhibition activity of the carrageenin induced paw edema in rats – they did not produce toxic effects in doses up to 0.5 mmol/kg body weight of the mouse. The experimental study enriched by theoretical experiments (molecular docking), suggested that compound **20b** was a potential anti-inflammatory agent.

2.2. Neurological disorders

Neural stem cells (NSCs) are characterized by multipotency, which means that they can differentiate into all the cells of the nervous system, the neurons and glial cells. NSCs are a source of nutrients and protection for damaged/dysfunctional cells, they have the ability to migrate to distant sites of injury secretion stimulated higher levels of SDF-1 by endothelial cells and astrocytes in the injured tissues (CXCR4 – SDF-1 receptor). Mammals possess little capacity to regenerate and repair the central nervous system. In adult mammalian neurogenesis *in vivo* occurs in the subgranular zone (SGZ) of the dentate gyrus of the hippocampus and the subventricular zone (SVZ) of the lateral ventricles of the brain. Because neurogenesis occurs continually throughout the adult's life, NSCs hold great promise for treating neurological disorders including multiple sclerosis, Parkinson's disease and Alzheimer's disease. To date, clinical applications of NSCs have not been successful. An alternative is the activation of endogenous neurogenesis and neuroprotection by chemical or genetic modification. Small molecules that can retard neuronal death or induce neurogenesis and neuroprotection are particularly interesting not only because of their therapeutic implications as novel therapeutic agents, but also because they can be used as an inestimable tool to study the mechanisms of neurogenesis.

One of the neurological disorder is Alzheimer's disease (AD), a progressive, degenerative disease of the central nervous system characterized by the existence of dementia, progressive deficits in cognitive functions and severe behavioral abnormalities, related to the disappearance of cerebral cortex. To date, there are no drugs retracting or stopping the progression of the disease. Pharmacological treatment consists of symptomatic treatment of memory disorders and cognitive functions. Currently, AD is increasing in people aged 65 years or elder and affects over 35 million people worldwide. The pathogenesis of AD has been found to be associated with numerous pathways including deficit in cholinergic functions [98], incorrect beta-amyloid protein metabolism and tau protein phosphorylation [99], and the connection inflammatory pathway and oxidative stress [100].

One of the widely accepted theories says that beta-amyloid (Aβ) peptides of 40 and 42 residues (Ab_{42} are more prone to aggregate than Ab_{40} or Ab_{38}) formed from the cleavage of amyloid precursor protein play a key role in AD pathogenesis [39,40]. The aggregation

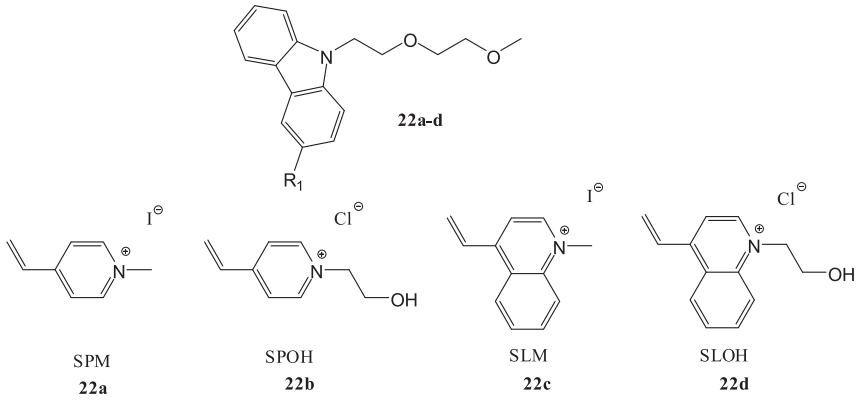

Fig. 11. Structures of carbazole-based cyanine dyes **22a**–**d**.

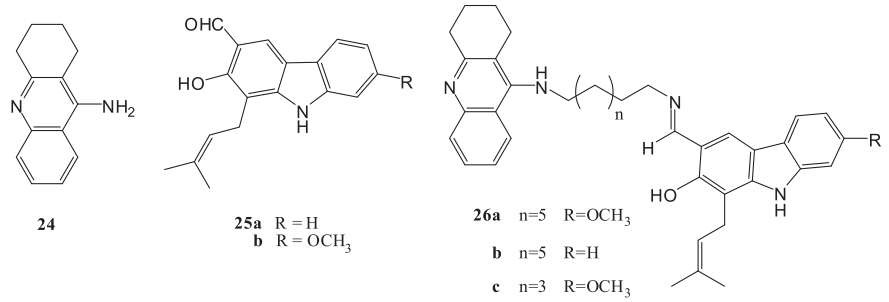

Fig. 13. Structures of tacrine–carbazole hybrids **26a**–**c** and starting substrates **24**, **25a**,**b**.

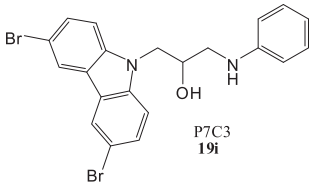

Fig. 14. Structure of aminopropyl carbazole P7C3 **19i**.

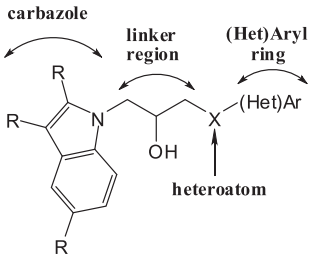

Fig. 16. Regions of P7C3 **19i** subject to modification.

of monomeric Aβ peptides to insoluble plaque also known as senile plaques may lead to the death of neuronal cells (on microscopic level plaques accumulate on the walls of blood vessels). The Aβ-peptides are generated by sequential processing of the amyloid precursor protein (APP) by β- and γ-secretase. The γ-secretase complex catalyzes the most important step in the liberation of these Aβ isoforms, and this can be a promising target for prevention of AD [39]. In recent years effective fibril inhibitors and β-sheet breakers that can prevent the aggregation of Aβ monomers into oligomeric and fibrillar conformations have been developed [40]. The tested compounds must show blood–brain barrier (BBB) permeability, low neurotoxicity and high *in vivo* stability to be clinically useful.

One of the tested inhibitors of Alzheimer β-amyloid fibril formation was the derivative of carbazole **21a** (Fig. 10) [41]. Compound **21a** known as CT is able *in vitro* to cross cell membranes and to penetrate rapidly inside the cells (it does not accumulate inside the mitochondria, but binds to DNA in the nucleus).

To track the accumulation of CT inside cells, the cellular models overexpressing P-gp and MRP1 (two proteins overexpressed in the blood brain barrier) were used. The blood brain barrier is a major impediment to the entry of many therapeutic drugs into the brain and these proteins help to protect the brain from the potential toxicity of exogenous compounds. The compound **21a** is a good P-gp substrate (its accumulation in P-gp overexpressing cells is very low), however is not an MRP1 substrate, which indicates that it will probably not pass through the blood brain barrier.

One of the compounds that can penetrate the blood–brain barrier, which makes it a potential neuroprotective and/or therapeutic agent for Alzheimer's disease, is SLOH **22d** [40]. It was shown to inhibit the aggregation of Aβ peptides and oligomers, thus preventing the fibril growth. In view of the potential clinical use, the cytotoxicity of four such compounds towards human neuroblastoma SH-SY5Y neuronal cells was evaluated. The cytotoxicity in a 10 nm, 1 μm, 10 μm, and 50 μm concentration for all compounds upon exposure for 2, 6, and 24 h was determined. What is more important, SLOH **22d** was non-toxic to the neuronal cells (cytotoxicity of SLOH < 20%, ≤ μM from 2 to 24 h of exposure, for the other **22a**,**b**,**c** < 35%) and exhibited a protective effect against the neurotoxic activities of Aβ oligomers and fibrils (Fig. 11).

On the basis of the theoretical claim that the Aβ-peptides are generated by sequential processing of the amyloid precursor protein (APP) by β- and γ-secretase Schmidt et al. synthesized new non-steroidal anti-inflammatory (NSAIDs) N-sulfonylated or N-alkylated carbazolyloxyacetic acids, structurally related to the substrate targeting γ-secretase modulator flurbiprofen [39]. The authors suggested earlier that the NSAID's carboxylic acid interacted with a basic amino acid, for example, lysine[624] on amyloid

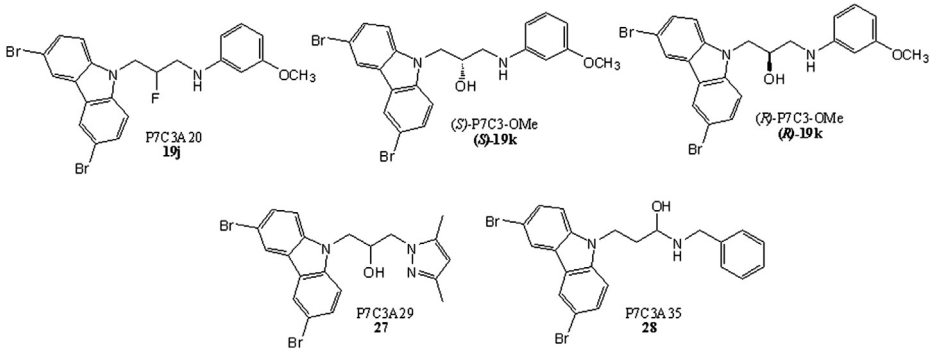

Fig. 15. Structural modifications of P7C3 **19i**.

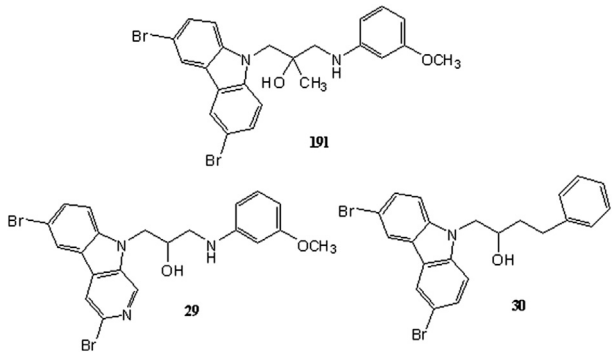

Fig. 17. Structural modifications of P7C3 **19i**.

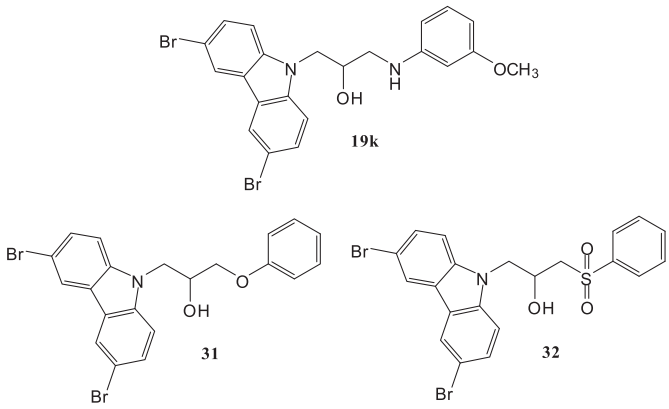

Fig. 18. Compounds prepared and tested in the form of pure enantiomers.

precursor protein (APP), which is located in the vicinity of GxxxG motif, at the membrane interface.

Two major structural elements of 33 new carbazole compounds are the substituents such as N-alkyl chain (enhances the modulator activity probably by modulator orientation via a membrane anchoring effect) and carboxylic acid isosteres (expected γ-secretase modulatory effects). Several established carboxylic acid isosteres such as tetrazole, sulfonic acid, amides, sulfone amides and tetronates were chosen. The effect of hydroxyl, amino and nitrile substituents was also studied. In addition, derivatives with bulky groups as sterical hindrance were obtained to investigate the modulator binding site. Because the beta-amyloid (Aβ) peptides of 42 residues ($A\beta_{42}$) are more prone to aggregate than the peptides of 38 and 40 residues ($A\beta_{38}$ and $A\beta_{40}$), the activity of the new compounds was tested for peptides of this length (IC_{50}/EC_{50}). Four different modes of actions in tested cellular assay were observed: γ-secretase modulation (increase in $A\beta_{38}$, decrease in $A\beta_{42}$), inverse γ-secretase modulation (decrease of $A\beta_{38}$, increase of $A\beta_{42}$), γ-secretase inhibition (decrease of $A\beta_{38}$, decrease of $A\beta_{42}$) and lack of activity, but the modulatory activity was detected only for acidic moieties and metabolically labile esters.

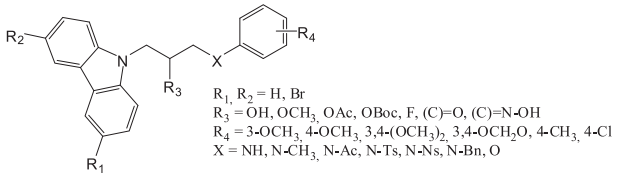

Fig. 19. Structures of aminocarbazole derivatives**19** and compound **31**.

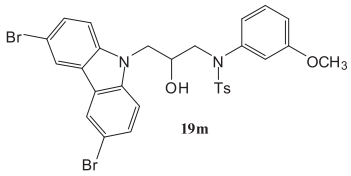

Fig. 20. Structure of N-tosylated aniline derivative **19m**.

Despite the literature reports of poor brain permeability of the carboxylic acids, the authors synthesized carprofen **23a** N-decyl derivative **23b** (BSc3041) (Fig. 12), which showed a slow but significant BBB permeation in APP_{swe} *in vivo* (IC_{50} $A\beta_{42}$ = 2.9 μM, IC_{50} $A\beta_{40}$ > 40 μM, IC_{50} $A\beta_{38}$ = 5.8 μM). A potential prodrug system based on short linear esters, which complements the BBB permeation of the free acid **23b** was identified [39].

One of the pathways of pathogenesis of AD is deficiency in cholinergic neurotransmission. Acetylcholinesterase (AChE) is a hydrolase that hydrolyzes one of the main neurotransmitter acetylcholine into choline and acetic acid residue. Since the end of 1990s, intense research work has been conducted on the fully reversible inhibitors of acetylcholine esterase, which is of profound significance in the treatment of Alzheimer's disease symptoms, mainly through improvement of the cholinergic transmission in the peripheral nervous system. Because ChE as well as oxidative stress are important targets for the treatment of AD, studies of tacrine **24**, the first cholinesterase inhibitor (ChEI) drug, approved by FDA for the treatment of AD as a multifunctional agent, were conducted. Tacrine was withdrawn from the market, because of its strong liver toxicity. However, for development of multifunctional anti-AD agents the tacrine scaffold is still used because of its high potency and low molecular weight [101]. Connection of tacrine with heptaphylline **25a** and 7-methoxyheptaphylline **25b** via the alkylenediamine side chain gave three new compounds **26a**–**c** (Fig. 13) [42]. All synthetic derivatives were explored for their biological activities to selected targets characteristic of AD: AChE, butyrylcholinesterase (BuChE), and antioxidant. These compounds have shown high inhibitory effect on AChE with IC_{50} values 0.48, 0.95 and 1.03 μM, respectively, and exhibited good inhibition selectivity against AChE over BuChE [IC_{50} (BuChE)/IC_{50} (AChE)], 108.6, 20.4, 62.4, respectively. The linker length between the carbazole ring and the tacrine moiety plays a significant role in determining the inhibitory activity for ChE as well as methoxyl group at the 7-position of the carbazole for inhibition selectivity against AChE over BuChE.

Compound **26c** with three methylene linker showed less potent ChE inhibitory activity than **26a** with the five-methylene linker. Compound **26a** with a methoxyl group at the 7-position of the carbazole moiety exhibited more potent AChE inhibitory activity than compound **26b** without this substituent (R = H, Fig. 13). However, for BuChE inhibitory activity, the presence of this substituent was unfavorable (R = OCH_3, Fig. 13). The derivatives **26a** and **26c** containing a methoxy group showed potent ABTS radical scavenging activity (IC_{50} 8.34 ± 1.68 and 9.77 ± 0.03 μM,

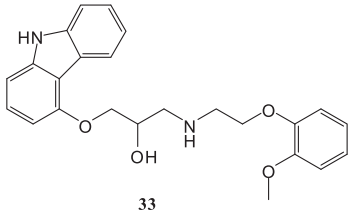

Fig. 21. Structure of carvedilol **33**.

respectively), while tacrine did not have this ability. The results indicate that derivatives **26a**–**c** can reduce neuronal death induced by oxidative stress and β-amyloid (Aβ). Compound **26a** also showed an ability to improve both short-term and long-term memory deficit in mice induced by scopolamine. Thus the new tacrine–carbazole hybrids seem to be possible candidates for further pharmacological study for Alzheimer's therapy.

An alternative way of AD treatment focused on promoting hippocampal neurogenesis. Recently, McKnight et al. have established that aminopropyl carbazole P7C3 **19i** showed proneurogenic and neuroprotective properties, stabilized mitochondrial membrane potential and inhibits newborn neuron apoptosis, corrected hippocampal deficits in mice devoid of adult neurogenesis and preserved cognitive capacity in aged rats (Fig. 14) [43]. They used computational methods for the selection of 1000 small molecules from a library of 200,000 drug-like chemicals, and conducted *in vivo* screening using mice lacking the ability of hippocampal neurogenesis.

Since the 1960s when the experimental evidence for the formation of new neurons in the hippocampal dentate gyrus, olfactory bulb and cerebral cortex of adult rats was given [102,103] it has been assumed that all mammalian species, including humans, harbor reservoirs of neuronal stem cells in the subgranular zone (SGZ) of the hippocampal dentate gyrus and the subventricular zone (SVZ) [104]. Recently, it has been found that a large subpopulation of hippocampal neurons, nearly one-third of the neurons, is subject to exchange. In adult humans, 700 new neurons appear in each hippocampus per day (1.75% of the neurons within the renewing fraction per year). It has been demonstrated that neurons are generated through adulthood and that the rates of their generation are comparable in middle-aged humans and mice. It suggests that adult hippocampal neurogenesis may contribute to human brain function [105]. P7C3 **19i** has the ability to suppress apoptosis of newborn hippocampal neurons, and enhance neurogenesis in aged rats, which was in silico predicted by ADME characteristics (Absorption, Distribution, Metabolism, Excretion) [43]. To evaluate its properties, an *in vivo* structure activity relationship (SAR) study was made using 37 chemical derivatives of this compound for the assessment of proneurogenic activity (Fig. 15). Most inactive modifications resulted from replacement of the aniline moiety with a pyrazole P7C3A29 **27** and elongation of the linker connecting the tricyclic carbazole to the aniline ring by a methylene group $-CH_2$-P7C3A35 **28.** Derivative P7C3A20 **19j** showed an increased activity when compared to that of the parent compound P7C3 **19i**. In this derivative a fluorine replaced hydroxyl group and the aniline ring of P7C3 was substituted by anisidine. The latter structural modification P7C3-OMe **19k** showed comparable properties to the parent compound P7C3 **19i**. The presence of a stereogenic center has opened the possibility of synthesis of P7C3-OMe analogs in enantiomerically pure forms. The *R*- and *S*-enantiomers (*R*)-P7C3A20 **(*R*)-19k** and (*S*)-P7C3A20 **(*S*)-19k** were synthesized, separated, and evaluated in the *in vivo* neurogenesis assay (Fig. 15). It was shown that the *R*-enantiomer preserved the extensive majority of proneurogenic activity and that it was far more active than the *S*-enantiomer [43].

Ready et al. conducted a systemic study of the new analogs of P7C3 **19i** and investigated the effect of the presence of carbazole ring, the linker region, heteroatom and heteroaromatic and aryl ring on their proneurogenic activities (59 analogs were tested in live mice) (Fig. 16) [44].

It appeared that the carbazole ring system was not required to achieve high activity. For example, β-carboline **29** was as active as **19i** (Fig. 17). However, the replacement of carbazole moiety by systems partially saturated (tetrahydro-γ-carboline) or smaller (dimethyl indole) resulted in a decrease in activity. The presence of bromines in **19i** (toxicity toward HeLa cells: GI_{50} = 5.1 μM, LC_{50} = 21.4 μM, half life in mouse hepatocytes > 240 min, half life in human hepatocytes > 240 min) is very important; several derivatives with different substituents (I, Cl, Me, CN) were obtained, but the ones with the two bromine substituents were the most effective.

The next stage of the research was to synthesize P7C3 **19i** analogs with the modified linker region. Several compounds showed increased activity after replacement of the hydroxyl group with a fluorine (N-methyl derivative, the sulfoxide-containing analogs, anisidine derivative) in other ones no such improvement was observed. Nevertheless, the most active compound from all derivatives was the fluorinated anisidine derivative **19j**. Another very effective modification was a conversion of P7C3 **19i** to a tertiary alcohol **19l** (toxicity toward HeLa cells: GI_{50} = 10.9 μM, LC_{50} > 30 μM, half life in mouse hepatocytes > 240 min, half life in human hepatocytes > 240 min) (Fig. 17). The modification of the linker region was beneficial when an additional methylene group was inserted between the hydroxyl group and the aniline, but not between the hydroxyl and the carbazole. To test the efficacy of alternative heteroatoms, several analogs were synthesized. What is interesting, aniline could be replaced with an aryl ether, thioether or a sulfone. While several heteroatoms appear acceptable at this position, an analog with only a hydrocarbon linker **30** was found to be not neuroprotective at the concentrations tested. Also several compounds with the modified right-hand aromatic fragment were synthesized. Simple NH_2- or O-alkyl-terminated compounds showed modest activity (Fig. 17).

Heteroaromatic rings proved less effective (pyridines, pyrazines, indoles, carbazoles, pyrazoles, triazoles) with two notable exceptions 2-aminopyridine and azapyridone. Additionally, several enantiomerically pure derivatives were tested: the anisidine analog of P7C3 **19k**, aryl ether **31** (**(S)-31** toxicity toward HeLa cells: GI_{50} = 10.3 μM, LC_{50} > 30 μM, half life in mouse hepatocytes > 240 min, half life in human hepatocytes > 240 min), and sulfoxide **32** (toxicity toward HeLa cells: GI_{50} = 16.1 μM, LC_{50} > 30 μM, half life in mouse hepatocytes 224 min, half life in human hepatocytes 43 min) (Fig. 18).

In all three cases tested, *S*-enantiomers showed higher activity and a significant difference in activity was observed between the respective pairs of enantiomers. The compounds discovered can be orally administered, are nontoxic, stable in mice, rats, and cell cultures. They are also capable of penetrating the blood–brain

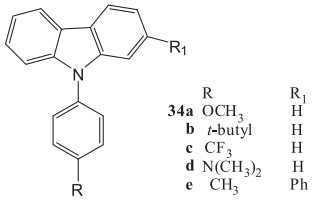

Fig. 22. Structures of N-substituted carbazoles **34a**–**e**.

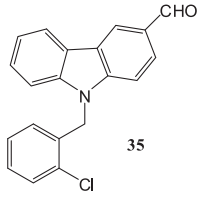

Fig. 23. Structure of LCY-2-CHO **35**.

barrier. The most potent compounds were found to be active at nanomolar concentrations.

Lee and co-workers have performed the synthesis and screening of 25 new aminopropyl carbazole derivatives (Fig. 19) [45]. On the basis of literature data the authors decided to analyze the effects of two types of modifications: at the 2-hydroxypropyl linker region and at the aniline ring (substituents R_3, R_4 and X, respectively).

The effective compounds, enhanced neuronal differentiation in conducted experiments, exhibited activity comparable to P7C3 **19i**.

Several N-substituted aniline derivatives (R_2 = CH_3, $COCH_3$, Ts) showed slightly higher activity than their amine analog **19k**. Further it appeared that 2-hydroxyl group was necessary for proneurogenic activity as its modification (R_3 = OCH_3, OAc, Br, C=O, C=N–OH, F) resulted in a decrease in activity (Fig. 19). Among the analogs tested, compound **19m** demonstrated an excellent proneurogenic and neuroprotective activity in NSCs, higher than P7C3A20 **19j**, with no detected toxicity (Fig. 20).

This compound also suppressed astrocytogenesis and proliferation of NSCs, thereby boosting overall survival of NSCs. The obtained results have provided some basic knowledge on the mechanisms of neuroprotective effect of the aminopropyl carbazole derivatives and also can help in the design of affinity probes to identify the molecular targets.

One of the compounds with the carbazole skeleton that influences neurological conditions by different mechanisms is carvedilol **33** (Fig. 21).

(±)-[3-(9*H*-carbazol-4-yloxy)-2-hydroxypropyl][2-(2-methoxyphenoxy)ethyl]amine **33** is a multiple-action drug: it is a nonselective α/β-adrenergic receptor blocker, recommended for the treatment of hypertension, ischemic heart diseases, chronic heart failure, arrhythmias and glaucoma. Carvedilol is a racemic mixture in which S-(−)-enantiomer has the ability to block nonselective β-adrenoreceptor, while α-adrenergic receptor is blocked by both R-(+) and S-(−)-enantiomers at equal potency. Its effectiveness in the treatment of cardiovascular diseases is mediated, in part, through its antioxidant and anti-inflammatory

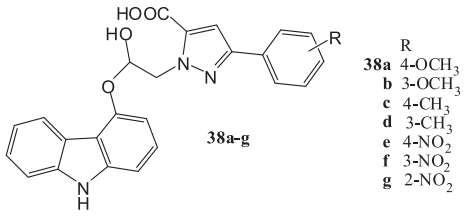

Fig. 25. Structures of 1-(30-(9H-carbazol-4-yloxy)-20-hydroxypropyl)-3-aryl-1H-pyrazole-5-carboxylic acid derivatives **38a**–**g**.

activities, depending on the carbazole moiety, which is characteristic of carvedilol [106,107]. Therefore, the antihypertensive drugs, including β-adrenergic blockers such as carvedilol, have been checked for a possible protecting effect against Alzheimer's disease [108,109]. It has been shown that due to its antioxidant properties carvedilol exhibits neuroprotective activity through different mechanisms [48,50,110–116]. *In vivo* studies have suggested that some drugs with such properties as carvedilol, could selectively protect against Alzheimer's disease by preventing the accumulation of oligomeric Aβ peptides [47]. Earlier studies had indicated that carvedilol has ability to bind Aβ-peptides and prevent Aβ from forming oligomeric fibrils because of the specific 3-dimensional pharmacophore conformation [117]. Recently, the use of carvedilol has been suggested to bring cognitive benefits in AD patients [108].

Pasinetti et al. in their research on the effects of carvedilol on neuronal transmission and long-term potentiation (LTP) used six month-old TgCRND8 mice and their B6C3F1 wild-type age-matched controls [46]. They have found that acute carvedilol treatment of hippocampal slices from TgCRND8 mouse model of AD, reestablished basal synaptic transmission, improved LTP, enhances neuronal plasticity and suppresses neuronal hyperexcitability as measured by epileptic discharge activity. These were the first studies on synaptic transmission and plasticity in a mouse

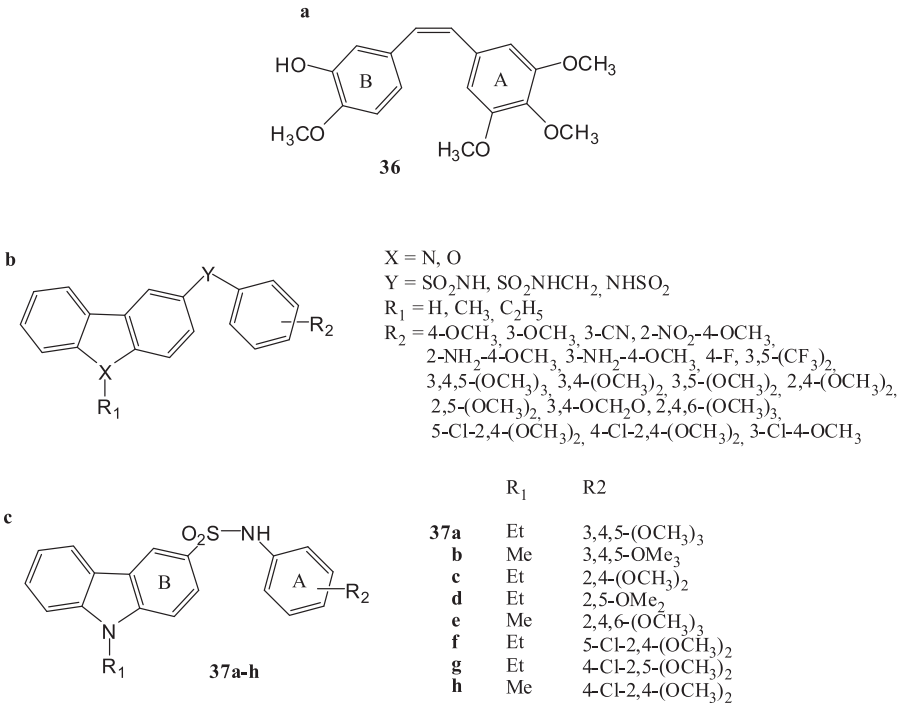

Fig. 24. (a) Structure of Combretastatin A4 **36**; (b) Structural elements of new carbazole sulfonamides; (c) Structures of the most active compounds **37a**–**h**.

model of AD, testing the effects of a nonselective α/β adrenergic receptor blocker, particularly carvedilol. In the later *in vitro* studies Pasinetti et al. have shown that carvedilol interferes with Aβ aggregation mechanisms [47]. To be more exact, they suggested that carvedilol interferes with Aβ peptide protein–protein interactions and in this way inhibits aggregations of Aβ peptides into structurally ordered neuropathological Aβ conformers. Carvedilol blocked almost completely oligomerization of $A\beta_{1-42}$ and also interfered with oligomerization of $A\beta_{1-40}$ in a dose-dependent manner. On the basis of these results the researchers studied the physiological relevance of carvedilol in AD by exploring the role of carvedilol in cognitive function and neuropathology using two independent AD mouse models TgCRND8 and Tg2576. Carvedilol, which easily crosses the blood–brain barrier was detected in the mouse brain and was well tolerated in both mouse models [118]. Oral administration in drinking water, 5 months of carvedilol treatment, did not cause adverse effects as unstable weight and altered blood pressure and heart rate. Carvedilol treatment improves cognitive function and basal synaptic transmission in the brains of AD mice.

Oxidative stress affects particularly easily the central nervous system (CNS) because, comparing to other organs, it is rich in highly oxygen-consuming polyunsaturated fatty acids. Besides, it shows a relatively low level of antioxidants and low regenerative capacity.

Carvedilol causes neuroprotective effect on 3-nitropropionic acid-induced neurotoxicity in N1E-115 neuroblastoma cells [48]. 3-Nitropropionic acid (3NP), a fungal toxin which is neurotoxic to animals and humans, is one of the factors causing oxidative stress and other molecular and cellular changes similar to those observed in neurons of patients with Huntington's disease. Huntington's disease (HD) is a neurodegenerative genetic disorder (defect on chromosome 4). The death of nerve cells in certain areas of the brain results in gradual loss of cognitive (thinking, perception, awareness, judgement), physical and emotional function. Early features can include personality changes, mood swings, nervous movements, irritability. The most common symptom is jerking of the arms and legs (called "chorea"). Carvedilol significantly reduced the high level of oxidative and cell necrosis in both protocols used in research (addition of drug before and after incubation with 3NP), but the effect was stronger when the drug was added before the damage was induced by 3NP. Carvedilol (10^{-5} M) suppressed the oxidative damage, reduced lipid peroxidation, total LDH activity, the depletion of reduced glutathione (GSH) and the reduction of antioxidative enzymes activities in N1E-115 cells incubated with 100 mM 3NP. The cytoprotective action of carvedilol was most likely associated with its antioxidative properties (connected with tricyclic carbazole moiety), which confirms the results of previous studies [119].

Fang et al. investigated the effect of carvedilol (3–20 μM) on oxidative stress-induced cell death by glutamate and H_2O_2 (2 mM and 600 μM, respectively) and the activity of Nrf2/ARE pathway in HT22 cells, an immortalized mouse hippocampal cell line [49]. An important cellular stress response involved in neuroprotection is the nuclear E2-related factor 2 (Nrf2)/antioxidant response element (ARE), which may become a potential therapeutic target in neurodegenerative disease [120]. Carvedilol significantly increased cell viability (10 μM almost fully preventing the damage) and

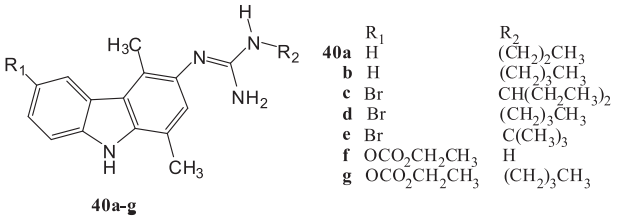

	R_1	R_2
40a	H	$(CH_2)_2CH_3$
b	H	$(CH_2)_3CH_3$
c	Br	$CH(CH_2CH_3)_2$
d	Br	$(CH_2)_3CH_3$
e	Br	$C(CH_3)_3$
f	$OCO_2CH_2CH_3$	H
g	$OCO_2CH_2CH_3$	$(CH_2)_3CH_3$

Fig. 27. Structures of N-(1,4-dimethyl-9H-carbazol-3-yl)-N′-alkylguanidines **40a–g**.

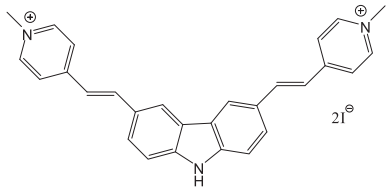

Fig. 28. Structure of 3,6-bis(1-methyl-4-vinylpyridium iodine)carbazole BMVC **41a**.

significantly decreased glutamate- and H_2O_2-induced reactive oxygen species (ROS) production in HT22 cells. Carvedilol significantly activated the Nrf2/ARE pathway and then up-regulated the expression of the protein levels of heme oxygenase-1 (HO-1) and NAD(P)H quinone oxidoreductase-1 (NQO-1), two downstream factors of the Nrf2/ARE pathway.

One of the contributing factors in the pathogenesis of neurodegenerative disorders may be aluminum, whose increased level is observed in the brain of patients with Parkinson's or Alzheimer's disease, amyotrophic lateral sclerosis. Kumar et al. studied the effect of carvedilol on memory performance in the Morris water maze task in aluminum treated rats [50]. They also studied the effect of carvedilol on lipid peroxidation, nitrite, reduced glutathione, glutathione S-transferase, superoxide dismutase, and catalase activity in whole brains of rats treated with aluminum chloride as well as effect of carvedilol on aluminum concentration and on acetylcholinesterase (AChE) activity in aluminum chloride treated rats. The results indicated that chronic treatment of aluminum chloride (100 mg/kg per day for six weeks) led to significantly increased cognitive dysfunction in the Morris water maze and to the oxidative damage as evidenced by the increase in lipid peroxidation and nitrite concentration and depleted reduced glutathione, superoxide dismutase, catalase and glutathione S-transferase activity compared to sham treatment. At the same time acetylcholinesterase activity and the aluminum concentration in brain significantly increased. Chronic administration of carvedilol (2.5 and 5 mg/kg per day for six weeks) not only significantly improved the memory retention but also reduced oxidative damage induced by chronic aluminum administration, indicating that carvedilol improves behavioral and biochemical functions of brain-treated aluminum.

Wen et al. have used N-substituted carbazoles for the biological

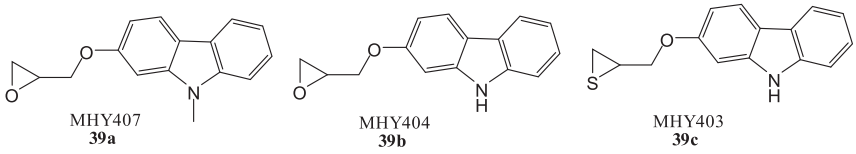

Fig. 26. Structures of carbazole derivatives with epoxypropoxy and thioepoxypropoxy moieties **39a–c**.

screening against the death of neuronal HT22 cells induced by neurotoxins including glutamate and homocysteic acid (HCA) [51]. Most important for the activity of the new compounds was the phenyl ring with bulky substituents on the carbazole nitrogen atom. The neuroprotective activity was significantly increased when such a group as methoxylphenyl **34a**, t-butylphenyl **34b**, trifluorophenyl **34c**, and N,N-dimethylaminophenyl **34d** was introduced, while N-alkyl substituted carbazoles (n-butyl, cyklohexyl, $(CH_2)_4OH$) showed none or low neuroprotective activity (Fig. 22). Several new carbazoles showed significant neuroprotective effect at the concentration of 30 μM, however only compound **34e** showed a similar activity at the concentration as low as 3 μM. This compound inhibits the proliferation but does not induce cell toxicity at 30 μM as established using LDH cell toxicity assay. It appeared that compound **34e** could be a model for testing and developing new drugs with potent neuroprotective activity against oxidative stress-associated CNS diseases such as AD (Fig. 22).

Oxidative stress is often the result of unregulated production of reactive oxygen species (ROS), e.g. nitric oxide (NO). Overproduction of NO by activated microglia cells, the resident macrophages in the central nervous system, plays a key role in neurodegenerative disorders. Wang et al. have synthesized and tested 9-(2-chlorobenyl)-9H-carbazole-3-carbaldehyde (LCY-2-CHO) **35** as a potential inhibitor of nitric oxide production (Fig. 23) [52]. The compound **35** was found to have no cytotoxic effect on microglia and suppressed the NO production on selected cell lines. Analysis of effects of LCY-2-CHO on NO production in microglial cells and many other processes have revealed these mechanisms.

2.3. Antitumor activity

The aim of most of the currently clinically used chemotherapeutic drugs is to kill malignant tumor cells by some of the mechanisms causing damage to the cell cycle and cell death or inhibiting cells growth and division. Apoptosis is the process of programmed cell death that occurs in multicellular organisms. When normal cells are damaged beyond repair they are eliminated by apoptosis. Cancer cells avoid apoptosis and divide in an uncontrolled manner. Disorders to apoptosis have been involved in the pathogenesis of many diseases including cancers. The huge growth of tumor cases has prompted the search for ways of eliminating excessively proliferating cancer cells. Some of them are the regulation of cell cycle and apoptosis. Because apoptosis can prevent the occurrence of inflammatory response, therefore synthetic carbazole derivative **35** identified as an anti-inflammatory compound was examined (Fig. 23). The comparison of the cell selectivity of LCY-2-CHO, showed that T-cell acute lymphoblastic CEM leukemia cells were sensitive to 1 mM LCY-2-CHO, acute myeloid leukemia HL60 cells underwent apoptosis at 10 mM of **35**, while cancer cells, as PC3, HT29 and MCF7, were resistant to 30 mM of **35**

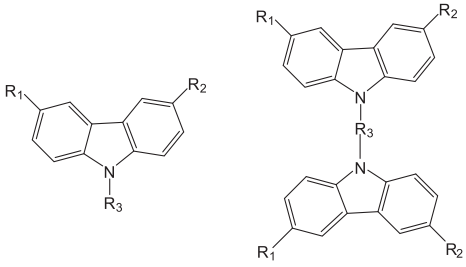

Compound	R_1	R_2	R_3
41a BMVC	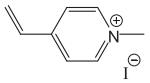		H
41b BMVC-8C			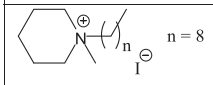
41c BrMVC	Br		H
41d $(MVC)_2$-8C	H		$-(C_8H_{16})-$
41e $(BMVC)_2$-8C			$-(C_8H_{16})-$
41f BMVC-4C			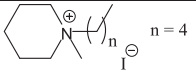
41g BMVC-5C	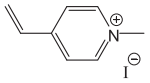	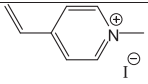	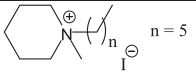
41h BMVC-9C			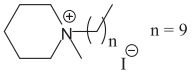
41i BMVC-12C			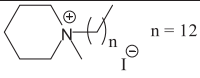
41j BMVC-8C3O			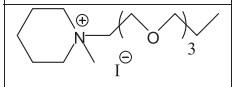

Fig. 29. Structures of BMVC derivatives **41b**–**j**.

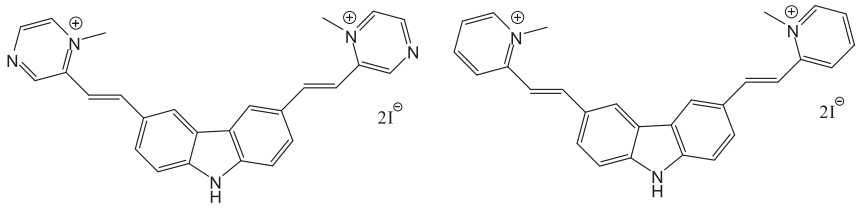

42 43

Fig. 30. Structures of BMVC analogs **42** and **43**.

within 24-h incubation. The tested compound showed apparently cytotoxic effect against the leukemia lines (CEM and HL60), but had little effect on the cell viability of PC3 (prostate cancer), HT29 (colon cancer) and MCF7 (breast cancer) cells. LCY-2-CHO **35** might be selectively cytotoxic against certain leukemia cells and apoptotic for malignant hematopoietic cells (the process is mediated through activation of caspase and mitochondrial pathways) [53].

The other factors leading to apoptotic cell death and tumor regression are antimitotic agents. Many of classic antimitotic agents are tubulin-binding ligands (e.g. taxanes, vinca alkaloids) that disturb the dynamics of micro tubules by targeting tubulin, this mechanism has been widely used to treat human cancers. Structure–activity relationship studies of Combretastatin A4 **36**, a small tubulin binding agent, isolated from the South African bush willow *Combretum caffrum*, have shown that the 3,4,5-trimethoxy substituents of the A-ring are necessary for good biological activities (Fig. 24a). Therefore, the attempts have been made at modifications of B-ring and changing the linking group to obtain analogs with better biological activities.

Boykin et al. have studied the influence of various substitutions on the A-ring, the effect of replacement of the olefin linker with sulfonamide groups and replacement of the B-ring unit with a carbazole in this new class of compounds [54]. The sulfonamide moiety was chosen because of biological activities (e.g. antibacterial, hypoglycemic) of sulfonamides drugs [121,122] and literature reports about the sulphonamides potential for inhibition of tubulin polymerization and antiproliferative properties.

In two series of carbazole sulfonamides (26 new compounds, Fig. 24b) thirteen of them exhibited IC_{50} values of < 1 μM against CEM leukemia cells (used for initial compound screening because of their known rapid proliferation and high sensitivity to standard anticancer agents). Eight of the new compounds **37a**–**h** exhibited strong activity against human leukemia cells (IC_{50} = 46–70 nM) (Fig. 24c). Five compounds **37a**–**d**,**g** were evaluated against a panel of eight human tumor cell lines: CEM (T-cell, leukemia, IC_{50} = 46–61 nM), Molt-3 (T-cell, leukemia, IC_{50} = 19–67 nM), Bel-7402 (hepatoma, IC_{50} = 96–219 nM), MCF7 (breast cancer, IC_{50} = 48–98 nM), DU145 (prostate cancer, IC_{50} = 144–603 nM), PC3 (prostate cancer, IC_{50} = 90–780 nM), DND-1 (melanoma, IC_{50} = 70–195 nM), DMS79 (lung cancer, tested only compounds **37a** and **37b**, IC_{50} = 1890 and 2088 nM, respectively). The compound 9-Ethyl-N-(3,4,5-trimethoxyphenyl)-carbazole-3-sulfonamide **37a** showed significant antitumor activity in two human xenograft models (MCF7 and Bel-7402). The results demonstrated that the nitrogen atom of carbazole and the alkyl substituent at position N-9 were very important for potent activity and cytotoxicity. The methoxy substitution and location on the A-ring have an important effect on cytotoxic activity. However, in contrast to compound **36**, where 3,4,5-trimethoxy substituents of the A-ring were required for potent biological activity (SAR informations), compounds had similar potent activities as 3,4,5-trimethoxy-substituted compounds **37a**,**b**. Replacement of methoxy group in ring A by a fluorine or chlorine atom enhanced the cytotoxicity. Preliminary studies with compound **37a** showed that the mode of action involves arrest of M-phase cell cycle and induction of apoptosis by increasing expression of p53 and promoting bcl-2 phosphorylation. Surprisingly, this derivative only weakly inhibited tubulin polymerization. These results suggest that the mode of action **37a** is different from **36** and involves an unidentified target(s). Carbazole sulfonamides are a novel promising class of antimitotic agents against solid tumors, potentially useful in clinical studies [54].

Another group of compounds which were screened to evaluate their cytotoxicity against cancer cells *in vitro* were the derivatives of 1-[3-(9H-carbazol-4-yloxy)-2—hydroxypropyl]-3-aryl-1H-pyrazole-5-carboxylic acid **38a**–**g** (Fig. 25) [55].

The activity of the compounds synthesized (used in various concentrations: 0.1, 1 and 5 mM for 48 h) was estimated by an SRB (sulforhodamine B) assay against cancer cells such as SK-N-SH human neuroblastoma (NB), human A549 lung carcinoma, and human breast cancer MCF7 cell lines. The most compounds showed significant cytotoxic effect against human SK-N-SH tumor cell line, isolated from a bone marrow taken from a four year-old girl with neuroblastoma. Neuroblastoma is a malignant tumor of neural tube cells (neuroblasts) most commonly diagnosed in infants. Compound **38a** and **38d** with 4-methoxy and 3-methyl substituent, respectively, were shown to significantly inhibit the growth of SK-N-SH cells. The compounds obtained were found useful for further investigation of the mechanism of cell proliferation, morphology, differentiation, and apoptosis.

Yoon et al. have used a new carbazole derivative MHY407 **39a** as a sensitizer of cancer cells to increase DNA damage, caused through the inhibition of topoisomerases as well as by inducing apoptosis (Fig. 26) [56]. The intention of the authors was to investigate the activity of the new compound in combination with DNA damaging anti-cancer agents such as doxorubicin, etoposide, or radiation. The compound MHY407 **39a** was selected from the other carbazole derivatives because of its DNA damaging ability greater than that of MHY404 **39b** and MHY403 **39c** (Fig. 26).

As shown in Fig. 26, the structure of carbazole was modified in positions 2 and 9. The addition of epoxypropoxy or thioepoxypropoxy groups at position 2 was designed to increase efficient cytotoxicity through DNA damage to cancer cells. It has been shown that MHY407 **39a** damaged DNA through a different mechanism (investigated in breast cancer cell lines MCF7 and Hs578T) than doxorubicin or etoposide. However, the co-treatment of breast cancer cell with MHY407 reduced cell viability and increased apoptosis, increased the formation of DNA damage-related proteins and foci. Thus MHY407 **39a** sensitized cancer cells to doxorubicin-, etoposide-, and radiation treatment via DNA damage.

Another group of carbazole compounds synthesized and tested for cytotoxic activity are guanidine derivatives **40a**–**g** (Fig. 27) [57]. Initially, the guanidines synthesized were screened for their cytotoxic activity against KB (nasopharyngeal epidermoid carcinoma) cell lines at concentrations of 10^{-6} M (0–26% antiproliferative activity) and 10^{-5} M (73–100% antiproliferative activity). Three

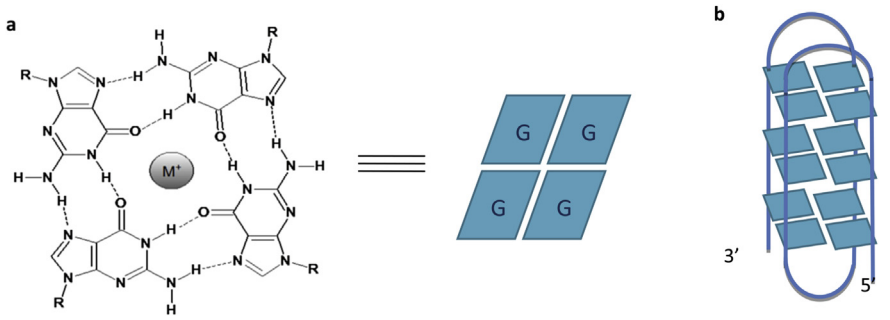

Fig. 31. (a) Diagram of guanine quartet structure; (b) Representation of intramolecular G-quadruplexes (basket structure).

derivatives **40c**, **40d** and **40e**, showed the relatively high inhibition values at a concentration of 10^{-5} M and they were also tested against HL60 cell line (acute promyelocytic leukemia) to give IC_{50} values 3.1, 3.5 and 4 μM, respectively. Since the derivative **40c** showed relatively the highest activity it was tested against cancer and non-cancer MCF7 (breast cancer), HCT116 (colon cancer), PC3 (prostate cancer) and MRC5 (lung fibroblast) cell lines and found to show potent antiproliferative activity against these cell lines at 10^{-5} M concentration.

Tumor-targeting therapy has appeared as an effective and attractive treatment of cancer. In recent years much attention has been focused on telomerase as one of various cancer specific targets tested. Telomerase is a ribonucleoprotein enzyme of multicomponent structure and increased activity in the stem cells (its activity decreases with age) and cancer cells, while telomerase activity is low or not detectable in the majority of somatic cells [123–125].

The activity of telomerase is related to the linear terminal fragments of chromosomes, the so-called telomeres. These structures are built of the invariable and repeatable sequence of nucleotides TTAGGG extending to the subtelomere region in which some changes in this sequence are observed. Telomeres do not code proteins, their function is to protect the terminuses of chromosomes against the loss of genetic information by preventing their gluing [126]. These rich in guanine structures undergo some small shortening upon each cell division, so the shorter the telomere the older the cell [127,128]. In the cancer cells, telomerase is active and maintains a constant length of the telomere DNA, so it guarantees the infinite number of the cell replications, making it practically immortal. For telomerase to be active, it must at first make a complex with a single-stranded section of telomere DNA at 3′ end, known as 3′-overhang. It has been proved that the single-stranded DNA having the repeated sequence (TTAGGG)n is able to form the four-stranded structure (G-quadruplex) not only *in vitro*, but also *in vivo* [129–131]. Folding into this specific "molecular knot" prevents formation of telomerase/DNA complex and hence prevents elongation of telomere, which should lead to death of the cancer cell after a certain number of divisions. The G-quadruplex structures are particularly favored in the presence of certain metal cations, e.g. K^+ and can be stabilized by specific ligands [92–97]. A large number of guanine-rich (G-rich) sequences are also found in the human genome [132,133].

One of the most studied to this date "G-quadruplex" ligands of carbazole skeleton is 3,6-bis(1-methyl-4-vinylpyridinium)carbazole diiodide (BMVC) **41a** designed and synthesized by Chang et al. (Fig. 28) [59].

BMVC does not cause acute cytotoxicity, it has been toxic to less than 15% of two human cancer cell lines of H1299 human lung cancer and Ca9-22 oral cavity cancer cells, and caused minimal damage to two normal fibroblast cell lines of the lungs MRC5 and the skin Detroit-551 cells after incubation with 0.5 μM BMVC for 72 h [59]. Unlike other telomerase inhibitors (IC_{50} = 0.05 μM), BMVC-treated cancer cells showed a fast telomere shortening rate and a lag period of growth before entering senescence. The cellular effects of BMVC were not limited to telomeres – BMVC also suppressed the tumor-related properties of cancer cells, including cell migration, colony-forming ability, and anchorage-independent growth [61]. Thus, BMVC repressed tumor progression through both telomere-dependent and telomere independent pathways. Because BMVC has a G-quadruplex stabilizing activity, G-rich regions within the promoter sequences of c-myc, VEGF, c-kit, BCL2, and KRAS proto-oncogenes (capable of forming G-quadruplex structures) could also be the target of this ligand [134–138]. Huang et al. have found that after incubation with BMVC, strong fluorescent signals could be detected in the nucleus of multiple human cancer cell lines but not in the corresponding normal cells (human normal lung MRC5 cells and human lung cancer CL1-0 cells were examined) [62]. To demonstrate how small ligands can selectively target specific subcellular organelles they synthesized BMVC derivatives **41b–j** with different physicochemical properties - their lipophilicity or hydrophilicity were increased by substituting a variable length alkyl linker and an N-methyl-piperidinium cation at the N-9 position of BMVC, respectively (Fig. 29).

They found that in normal cells BMVC is retained in the lysosomes, while in cancer cells it is localized in the mitochondria or the nucleus, where it binds to DNA (highly increased intensity of BMVC fluorescence). Lysosomes play an important role in intracellular degradation of endogenous and exogenous macromolecules, so they have appeared as a major target for drug delivery and have different properties in normal and cancer cells (e.g. in cancer cells pH is often higher and membrane permeability is perturbed). According to the structure–function analysis of BMVC derivatives, the hydrogen-bonding capacity (HBC) is a key determinant of lysosomal retention in normal cells. In cancer cells these derivatives are directed to the mitochondria or the nucleus by lipophilicity. HBC inversely correlates with permeance and oil–water partition coefficient.

Another carbazole derivative 3,6-bis(4-methyl-2-vinylpyrazinium iodide) carbazole BMVC4 **42** selectively inhibited telomerase activity *in vitro*, induced progressive telomere shortening and caused senescence in telomerase-positive cancer cells (Fig. 30) [63]. Telomerase inhibition might not be the primary cause of BMVC4-induced senescence. It has been shown that BMVC4 **42** also targeted a G-quadruplex forming sequence (QFS) located at the promoter region of c-myc and reduced its expression. BMVC4 **42** induced senescence in both telomerase-positive and telomerase negative ALT (alternative lengthening of telomeres) cancer cells (inhibition of telomerase IC_{50} = 0.2 μM). Ortho-isomer of BMVC, o-BMVC **43**, is good G4 stabilizer as BMVC [64], but a better G4 fluorescent probe with greater ability to distinguish G4 structures from duplexes (Fig. 30) [65].

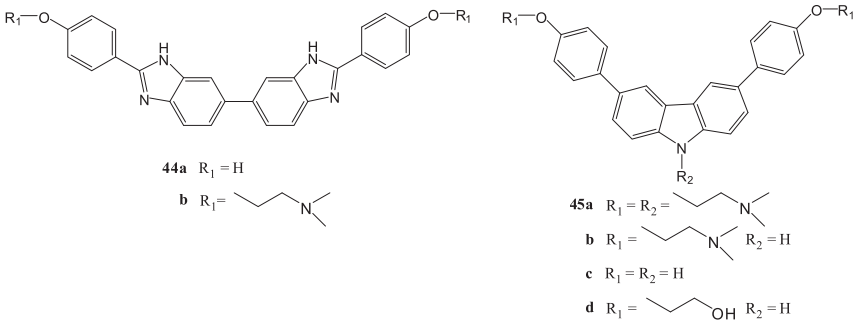

Fig. 32. Structures of bisphenylbenzimidazoles **44** and bisphenylcarbazole derivatives **45**.

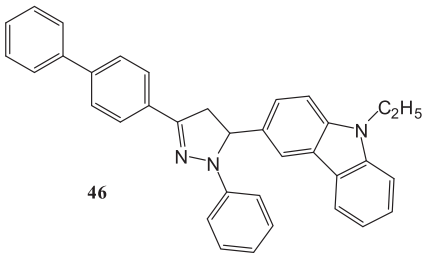

Fig. 33. Structure of 1-phenyl-3-biphenyl-5-(N-ethylcarbazole-3-yl)-2-pyrazoline **46**.

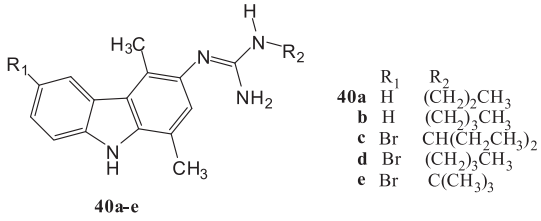

Fig. 34. Structures of N-(1,4-dimethyl-9H-carbazol-3-yl)-N′-alkylguanidines **40a**–**e**.

This is particularly important at the location of endogenous G4 structures in living cells using a fluorescence probe such as BMVC, because of the many duplexes in living cells it must be able to discriminate the small amount of G4 structures. The o-BMVC **43** is mainly distributed in the cytoplasm of human CL1-0 lung cancer cells and less in the nucleus. In contrast, BMVC **41a** is mainly located in the nucleus and less in the cytoplasm, probably due to its low lipophilicity. The photo-induced antitumor effect of BMVC *in vitro* and *in vivo* has been also studied [66]. Photodynamic therapy (PDT) is an effective treatment of cancerous and precancerous lesions. It can be repeated at the same site if necessary, and it is less destructive than traditional surgery. PDT requires specific photosensitizers (PSs) that are activated by specific wavelengths of light. Although it shows potential advantages in clinical application, PDT has several limitations that hinder its wide clinical acceptance. Among them the two main problems are sustained as skin photosensitivity and low tumor selectivity for PSs. *In vitro* cell line studies showed that BMVC significantly killed TC-1 tumor cells at light dose greater than 40 J/cm^2. *In vivo* tumor treatment studies showed that BMVC and light irradiation (iPDT) significantly inhibited the tumor growth (animal model). Cellular cytotoxicity of BMVC was evaluated in TC-1 cell line. The results obtained showed that BMVC may be a potent tumor-specific photosensitizer for photodynamic therapy.

Further studies have shown that free BMVC molecule is found both in the nucleus and mitochondria, whereas complexes of BMVC with guanine-rich oligonucleotides (GRO) are found mainly in either mitochondria or lysosome after cellular uptake in CL1-0 living cells, in MCF7 breast cancer cells and HeLa cervical cancer cells [67]. This indicates that cellular localization of GROs studied is not cell type-dependent. It has been indicated that GROs could act as a carrier to manipulate drug delivery to specific organelles. This creates the possibility of novel approaches to cancer treatment, particularly with mitochondria as a major target of cancer treatment.

Chang et al. described a very simple, cheap, rapid and non-invasive method for point-of-care screening cancer cells (an MRC-5 human lung fibroblast, an H1299 human lung cancer, an NIH3T3 mouse embryonic fibroblast, a CL1-0 human lung cancer were tested) based on the fluorescence analysis of BMVC [68]. The method based on BMVC fluorescence analysis is expected to substantially accelerate the clinical analysis of samples obtained from tissue biopsy, needle biopsy, or bodily fluids, etc. The diagnostic accuracy of this simple method in clinical tests on fine needle aspirates of neck masse is *ca.* 80%. The combination of the BMVC test and the fine needle aspiration (FNA) cytology has decreased the

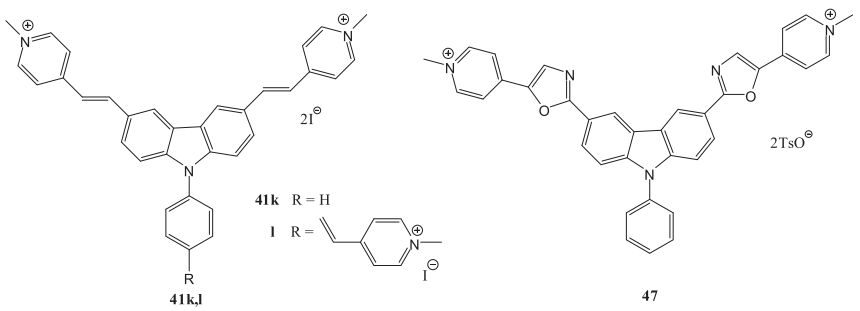

Fig. 35. Structures of N-phenylcarbazole derivatives **41k,l** and **47**.

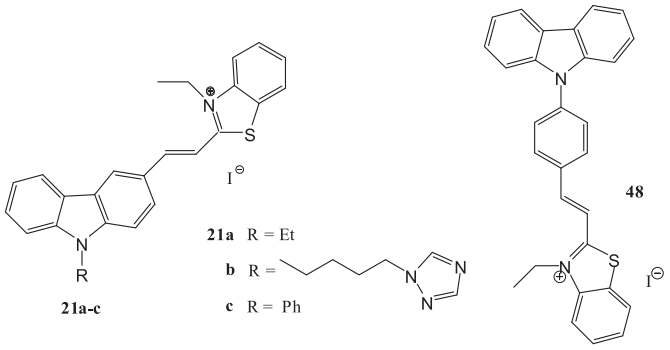

Fig. 36. Structures of vinylbenzothiazolium derivatives of N-substituted derivatives of carbazole **21a–c**, **48**.

undiagnosed cases by 65%. Moreover, an algorithm has been developed to improve the diagnostic accuracy of malignant neck lumps up to nearly 100% [69]. Early diagnosis of cancer greatly increases the patient's chances of recovery. BMVC was tested *in vitro* as a probe capable of detecting cell transformation, which may increase such a success [70]. BMVC has been applied to living cells in several different models of cell transformation, and the fluorescence signals of BMVC detecting formation of foci, significantly increased cellular motility, cell proliferation, cell apoptosis, anchorage-independent growth, and increased invasiveness of transformed cells. The results obtained have shown that BMVC probes are promising for early detection of cancer. Recently BMVC has been tested as an improved fluorescence assay for detection of malignant pleural, which diagnosis is an important issue in the management of malignant effusions [71]. The method named "BMVC test" has been developed to improve cytological tests at low cost. Comparing with results from double-blind cytologic examination, this simple test gives a good discrimination between malignant and benign specimens with sensitivity of 89.4% and specificity of 93.3% for diagnosis of malignant pleural effusion. BMVC test provides accurate results in a short time period, and the digital output could assist cytological examination to make it more objective and clear-cut. Also recently the activity of BMVC **41a** and BMVC4 **42**, as G-quadruplex structure stabilizers, have been tested on G-rich sequences located at the WNT1 promoter region, capable of forming G-quadruplex structures in the presence of potassium ion. WNT1 encodes a multifunctional signaling glycoprotein that is highly expressed in several malignant tumors. Patients with Wnt1-positive cancer are usually expected to have advanced metastasis [72]. Both ligands repressed the expression of WNT1 in a G-quadruplex structure-dependent manner. Upon the addition of BMVC and BMVC4 to cancer cells, the Wnt1-mediated signaling pathway was suppressed. Consequently, the migration and invasion abilities of cancer cells were also decreased. The results show that tumor metastasis can be suppressed as a result of stabilization of the G-quadruplex forming sequence located at the WNT1 promoter. This creates opportunities for new drug development to inhibit migration and invasion of cancer cells.

2.4. Interaction with DNA

Completion of Human Genome Project has brought about great interest in the ligands entering into specific interactions with DNA, both in the biomedical aspect (new formulations and strategies for treatment of cancer, viral infections or genetic diseases) and bioanalytical aspect (detection and diagnostics of DNA sequences). Usually, for verification of potential candidates for antibacterial and antifungal drugs, the interactions with double-stranded DNA have been tested. However, recently the study has been extended into stabilization of guanine quadruplexes (G-quadruplexes, G4 DNA). These structures form on the nucleic acid sequences rich in guanine residues and containing G-quartets (each consists of four guanines held together by eight hydrogen bonds) (Fig. 31a). G-quadruplexes are formed by association of two or four separate strands of DNA (intermolecular quadruplex) (Fig. 31b) or by rolling up a single strand (intramolecular quadruplex) with parallel or antiparallel orientation [92,94–96,139].

It is believed that the therapeutic effectiveness of such ligands in treatment of neoplasmic diseases is attributed to inhibition or poisoning of some DNA enzymes, in particular topoizomerases and telomerase [92,94,96,139–145].

Topoizomerases are the enzymes which *in vivo* unfold the double DNA helix to make the matrix accessible to replication or transcription enzymes. Depending on the number of simultaneously broken phosphodiester bonds, one can distinguish topoisomerase I – governing hydrolysis of a single bond so a cut of one strand and removal of supercoils from DNA, and topoisomerase II governing hydrolysis of two bonds, a cut of two strands. The ligands stabilizing quadruplex structures are capable of inhibition of telomerase *in vitro* [92,94,96,139,140,146]. The G-quadruplex structures are particularly favored in the presence of certain metal cations, e.g. K^+ and can be stabilized by specific ligands [92,94,96,139,140,147]. It is expected that the interest in these structures will increase following the verification of the hypothesis of G-quadruplexes formation *in vivo* [129–131]. The importance of G-quadruplexes is associated not only with the protection of the ends of chromosomes for human telomeres, but also in the regulation of gene expression for several gene promoters. The G-rich region within the promoter sequences of c-myc, VEGF, c-kit, BCL2, and KRAS proto-oncogenes was capable of forming G-quadruplex structures [134–138].

In order to improve the efficiency of specific binding to DNA and increase the selectivity of enzyme inhibition of microorganism, new compounds have been searched for. Over the last few years, the research work stimulated by attractive properties of carbazole derivatives, such as antibacterial, antifungal, anti-inflammatory ones has been mainly focused on the interactions with double-stranded DNA structures, in the hope of development of new drugs. It is generally believed that the mechanism of drug activity against different infections (e.g. opportunistic infections) is associated with the minor groove interaction with DNA sequences rich in AT bases. Organic compounds that bind in the minor groove of DNA typically have extended conjugated systems with unfused aromatic rings that are directly bonded (such as DAPI, Hoechst 33258, furamidine) or are connected through conjugated systems (such as netropsin, distamycin, berenil, and stilbamidine). Carbazole ligands bind to the minor groove of AT-rich sequences, although they contain flat chromophore, which is generally characteristic of the compounds intercalating to DNA. Such compounds could in principle bind to AT sequences by intercalation, but the minor-groove interactions in AT sequences are favored, and the binding energy minimum is reached for the interaction with the

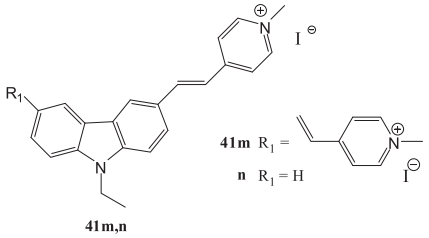

Fig. 37. Structures of N-ethyl modifications of BMVC.

minor groove rather than for the intercalation complex.

The observation that a drug can bind to the minor groove of AT sites and intercalates at GC sites is relatively rare but however, not new. Precedent cases have been reported, for examples, with the bis-benzimidazole derivative Hoechst 33258, lexitropsin, berenil or diamidino-diphenylfuran derivative DB60 [148,149]. In fact, the sequence dependent mode of binding to DNA first shown with the drug DAPI (4′,6-diamidino-2-phenylindole) which fits into the minor groove at AT sites and forms nonclassical intercalation complexes at sites where the GC pairs are highly propeller twisted so as to adapt to the shape of the inserting molecule [150–152].

Encouraged by the literature reports on the synthesis of a new class of head–head bisphenylbenzimidazoles **44** (with the hydroxyl moiety or with the dimethylaminoalkoxy chain), with promising antitumor properties and strong cytotoxic activity involving selective binding to the minor groove rich in sequences AT, Bailly et al. synthesized a series of compounds in which the bisphenylbenzimidazole moiety was replaced by a carbazole skeleton (Fig. 32) [73]. In studies of DNA interaction with four bisphenylcarbazole derivatives **45** it has been noted that the introduction of the two dimethylaminoalkoxy substituents increased the interaction of compounds with different DNA sequences. Their removal or replacement by the hydroxyl groups strongly diminished the interaction with DNA, and the addition of a third cationic side chain to the carbazole nitrogen increased the affinity of the compound to DNA. Bisphenylcarbazole derivatives are original pharmacophores that recognize DNA. The branched structure with two or three dimethylaminoalkoxy arms, because of their structural diversity, is an interesting skeleton to build molecules discriminating different conformations of nucleic acids.

Another compound with a structural element of carbazole examined for the interactions with single- and double-stranded DNA has been ligand **46** (Fig. 33). This derivative contained in its structure a second important structural element in the form of pyrazole moiety. 2-Pyrazolines are well known compounds with high fluorescence quantum yield and widely used in various fields (bleaching reagent, in photography as sensitizers, redox indicators, biological stains, laser dyes, fluorescence probes). In recent years, pyrazoline derivatives because of its unexplained to this date mechanism of biological activities have attracted the attention of researchers in the field of medicine (antibacterial, anti-inflammatory and antihypertensive activity). Therefore, Dong et al. used a derivative of pyrazoline with carbazole substituent (additional fluorophore) for studying the interactions with DNA [74]. As expected, the increase in fluorescence intensity of the ligand was observed with the ssDNA and ctDNA (single-stranded and calf thymus DNA, respectively) and further experiments showed that the new compound interacts with ctDNA by intercalation of carbazole substituent. The results of a pilot study encouraged the authors to synthesize modified pyrazoline ring analogs, in which part of the molecule was capable of rotating freely outside the helix, and study their interactions with DNA.

Another group of compounds having DNA binding properties are guanidines derived from carbazoles **40a**–**e** (Fig. 34) [57]. It has been established that fluorescence of all compounds strongly decreases in the presence of increased concentration of ctDNA. Derivative **40c** which shows the strongest biological activity (potent antiproliferative activity against HL60, MCF7, HCT116, PC3, and MRC5 cell lines at 10^{-5} M concentration) also has the best DNA binding properties from among all the derivatives tested.

The binding of the carbazole picric acid adduct (CP) **7** with ctDNA was characterized through UV–Vis spectrophotometry (Fig. 3) [35]. The absorption spectrophotometric titration results have shown that upon addition of increasing amount of ctDNA, a significant hypochromism is observed. This may indicate a strong interaction between double-stranded DNA and compound **7**, what, according to the authors, indicates intercalation binding mode.

Teulade-Fichou et al. have studied the binding preferences of three N-phenylcarbazole derivatives **41k**,**l** (Cbz-2Py and Cbz-3Py, respectively) and **47** (Cbz-2Ox5Py) to various DNA structures and sequences, especially in regard to the impact of N-phenyl substituent on DNA interaction (Fig. 35) [75].

Two of them are N-phenyl modifications of the known “G-quadruplex” ligand BMVC **41a**, which is able to stabilize G-quadruplex structures [82–87]. The derivatives differ in the number of methyl-vinylpirydynium arms, which is known to strongly influence their fluorescent properties. The linker was modified and replaced by an oxazole (Cbz-2Ox5Py **47**) in order to get the information on impact on the switchable fluorescence that characterizes the vinylic compounds. The vinylic derivatives showed strong fluorescence enhancement when bound to various double- and four-stranded DNA sequences while the oxazole derivative did not show such amplification in the presence of DNA. For ligand **41k** the structural preference for duplex vs. quadruplex is strongly dependent on the sequence of the duplex (particularly strongly bound to the minor groove of AT-rich sequences), while compound **41l** with three branches is not selective in relation to the examined structures (also bound to AT duplex but with a lower fluorescence enhancement). The test compounds showed no ability to *end stacking* stabilization of G-quadruplexes because of the steric hindrance of the N-phenyl core in contrast to the NH analog of BMVC **41a**.

Juskowiak's research group have synthesized new ligands and examined their affinities to different forms of nucleic acids for the biomedical and bioanalytical purposes. Before, they have studied the interactions of the new compounds with ctDNA and 22-mer four-stranded oligonucleotide of the human telomeric DNA sequence d[$AG_3(T_2AG_3)_3$] (22HTel), because of the possibility of using the novel compounds in biological research, in particular the inhibition of telomerase [153–155]. Recently, a subject of their interest has shifted to the ligands having a carbazole skeleton **21a**–**c**, **48** containing heterocyclic benzothiazolium moiety, the double bond C=C and additional substituents. All these structural elements of the compounds may affect their potential biological properties (Fig. 36) [76–80].

All the obtained compounds interacted with two- and four-stranded structures of nucleic acids, which was evidenced by distinct spectral changes. In the absorption spectrum of ligand **21b** a bathochromic shift and the appearance of hypochromic effect with isosbestic point were observed. These spectral changes are typical for intercalators, which indicated that the carbazole derivative tested interacted with ctDNA by intercalation, while in the four-stranded oligonucleotide of the human telomeric DNA sequence 22HTel we have to deal with layered *end-stacking* interactions. In the case of ligands **21a** and **21c** there is the possibility of binding in two or more different ways. All free ligands exhibited fluorescent properties, and after their binding to the DNA the fluorescence intensity increased significantly. Ligands **21a**–**c**, **48** stabilized structures of G-quadruplexes as evidenced by circular dichroism spectra, but have no effect on thermal stability of quadruplexes as almost no change in the melting point of G-quadruplex-ligand complexes was observed. Much higher affinity of all tested ligands to the three- and four-stranded structures with a significant preference for 46 mer d[$AGGG(TTAGGG)_7$] oligonucleotide with human telomere sequence (two G4 units connected by one TTA linker – *beads-on-a-string* model) and 18 mer of c-MYC oncogene sequence d($AG_3TG_4AG_3TG_4$) with tetraplex were noticed. Thanks to the structural element in the form of the double bond C=C, the ligands may undergo *cis-trans* photoisomerization. Preliminary experiments have shown that this is a complicated and

ambiguous process requiring further study. Pilot experiments on cytotoxicity of brest cancer cells MCF7 and MDA-MB-231 made for ligands **21a** and **21b** have shown that the compounds differ in activity (IC_{50} = 1.2 μM, 2.3 μM and 2.7 μM, 6.9 μM, respectively, for tested cell lines after 72 h of incubation) [81].

One of the most studied to this date "G-quadruplex" carbazole ligands is 3,6-bis[2-(1-methylpyridinium)vinyl]carbazole (BMVC) **41a**, which exhibits excellent ability to inhibit telomerase activity (IC_{50} = 0.05 μM) [59–72,82–89]. BMVC recognizes specific quadruplex structures, particularly the quadruplex of human telomeric sequence $d(T_2AG_3)_4$ (24HTel) and stabilizes it thermally. The fluorescence of BMVC can be used to discriminate between duplex and quadruplex DNAs [82] because, although the fluorescence of BMVC increases significantly in the presence of DNA, BMVC has high sensitivity and binding preference to quadruplex $d(T_2AG_3)_4$ over linear duplex $[d(GCATATGGCCATATGC)]_2$ (LD16) DNA. The fluorescence of BMVC was detected around 575 nm for quadruplex $d(T_2AG_3)_4$ (in the mixtures of 2 nM BMVC with the chromosomal DNA extracted from human cells) and at 545 nm for duplex LD16. These fluorescent properties of BMVC have been verified in the presence of G4 structure in native human telomeres [83,84]. BMVC binds to the G4 structure of 24HTel through external stacking to the end surface of G-quartet [85,86]. Experimental studies have shown a ~2:1 binding ratio of BMVC to H24 in both Na^+ or K^+ solutions. Molecular modeling confirmed that the most stable binding mode is the 2:1 binding model involving external stacking of BMVC to both ends of G-quadruplex of $d[AG_3(T_2AG_3)_3]$ (22HTel) [86]. BMVC stabilizes G4 quadruplexes via *end-stacking* interaction (the π–π stacking) and the electrostatic interaction between the positive charge of pyridinium moiety of ligand and the negative charge of phosphate groups of DNA. Further studies of molecular dynamics simulations have shown that the carbazole moiety and one pyridinium ring of BMVC are placed between the loop bases and the end surface of G-tetrad. The other pyridinium ring is bent to interact with the loop of G-quadruplex [86]. Loops play a key role in determining the nature of the folding and stability of G-quadruplexes. They along with tails of ligands could be essential for ligand binding [156,157]. It would be possible to distinguish structural isomers and to determine the binding modes of different G4 structures by substituting a base or varying the length and sequences of the loop. On the basis of different loop interactions at their binding sites it could be possible to distinguish different G4 structures making use of the induced CD patterns of BMVC. Although 10 years have passed since the synthesis of the ligand, BMVC is still a very promising object of research with really great potential use in anticancer therapy.

Including the current research into the binding mode between carbazole derivatives and G-quadruplex formed by human telomeric sequence, the following two carbazole compounds, derivatives of BMVC (3,6-Bis-(1-methyl-4-vinylpyridium iodine) 9-ethyl-carbazole) BMVEC **41m** and (3-Bis-(1-methyl-4-vinylpyridium iodine) 9-ethyl-carbazole) MVEC **41n** were synthesized and used in the study with parallel and antiparallel G-quadruplexes of the human telomeric DNA sequence $d(T_2AG_3)$ (6HTel) and $d(AT_2G_3T_2AG_3)$ (22HTel) (Fig. 37) [88].

It has been shown that the number of the cationic charges (pyridinium rings) in ligands plays a crucial role in stabilizing and binding mode of the human telomeric G-quadruplex structures. BMVEC **41m** having two cationic charge side groups of pyridinium rings can stabilize the parallel G-quadruplex of 6HTel by the end stacking onto the G-tetrad and groove binding mode. It can also increase the stabilization of antiparallel G-quadruplex of 22HTel by groove binding mode. MVEC **41n** having one cationic charge side group of pyridinium ring only can bind with the parallel G-quadruplex of 6HTel by the stacking onto the G4 G-tetrad and cannot interact with the G-quadruplex of 22HTel.

3. Conclusions

In recent 10 years, numerous carbazole derivatives have been synthesized and subjected to studies with various biological activities. Some of carbazole compounds have a very high activity against many organisms: bacteria, fungi, parasites, or are potential anti-inflammatory agents. The antimicrobial and antifungal activities of different compounds, including macrocyclic diamides and azoles based on carbazole skeleton, have been tested against many human pathogenic bacteria and fungi. Some of the compounds showed comparable or even better antibacterial and antifungal properties against tested strains than the reference drugs. A series of Incentrom A analogs, small molecules that perturb functions of specialized chromosomal structures called the centromere, that inhibit the chromosome segregation process in yeast have been synthesized and tested for their effects on chromosome stability and cell proliferation. Being incorporated into research on new antimalarial drugs, the 1-(1-aminopropan-2-ol)carbazole analogs were identified as potent drugs against *P. falciparum* K1 strain, responsible for most of the death caused by malaria.

Some derivatives of carbazole are potential multifunctional agents for the treatment of neurological disorders, including multiple sclerosis, Parkinson's disease and Alzheimer's disease (AD), and they act according to many different mechanisms. Small molecules that can retard neuronal death or induce neurogenesis and neuroprotection are particularly interesting not only because of their therapeutic implications as novel therapeutic agents, but also because they can be used as an inestimable tool to study the mechanisms of neurogenesis. The novel aminopropyl carbazole derivatives have been discovered as proneurogenic and neuroprotective chemicals. Because the pathogenesis of AD has been found to be associated with numerous pathways including deficit in cholinergic functions, incorrect beta-amyloid protein metabolism and tau protein phosphorylation, and the connection inflammatory pathway and oxidative stress, carbazole derivatives hold potential for the treatment of Alzheimer's disease by modulation of γ-secretase activity, acetylcholinesterase inhibition, reduction of neuronal death induced by oxidative stress and Beta-amyloid (Aβ) peptides, inhibition of formation and aggregation of these peptides.

The aim of most of the currently clinically used chemotherapeutic drugs is to kill malignant tumor cells by some of the mechanisms causing damage to the cell cycle and cell death or inhibiting cells growth and division. The huge growth of tumor cases has prompted the search for ways of eliminating excessively proliferating cancer cells. Some of them are the regulation of cell cycle and apoptosis. Some derivatives of carbazole show strong or moderate antitumor activity against different cell lines by a variety of mechanisms. Among them are carbazole sulfonamides, a novel promising class of antimitotic agents against solid tumors, potentially useful in clinical studies, carbazole derivatives with pyrazolecarboxylic acid, epoxypropoxy and thioepoxypropoxy or guanidine moieties.

Tumor-targeting therapy has appeared as an effective and attractive treatment of cancer. In recent years much attention has been focused on telomerase, a ribonucleoprotein enzyme of multicomponent structure, as one of various cancer specific targets tested. In cancer cells telomerase is active and maintains a constant length of telomeric DNA, the linear terminal fragments of chromosomes, which guarantees unlimited number of replications of the cell making it practically immortal. However, for telomerase to get active it must first make a complex with single-stranded fragment of telomeric DNA (3′-overhang). It has been proved that the single-stranded DNA having the repeated sequence (TTAGGG)n is

able to form the four-stranded structure (G-quadruplex) not only *in vitro*, but also *in vivo* and acts as a plug, preventing the complex formation with telomerase and hence telomere extension. Consequently, the cancer cell should die after a certain number of divisions and cancer development should stop. G-quadruplex structures are particularly favored in the presence of certain metal cations (e.g. K^+) and can be stabilized by specific ligands. Certain carbazole derivatives interact with different forms of nucleic acids and some of these are able to stabilize G-quadruplex structures. One of the most studied to this date "G-quadruplex" ligands of carbazole skeleton is 3,6-bis(1-methyl-4-vinylpyridinium)carbazole diiodide (BMVC). The cellular effects of BMVC were not limited to telomeres – BMVC also suppressed the tumor-related properties of cancer cells, including cell migration, colony-forming ability, and anchorage-independent growth. Thus, BMVC repressed tumor progression through both telomere-dependent and telomere independent pathways. Additionally, on the basis of fluorescence analysis of BMVC a very simple, cheap, rapid and non-invasive method for point-of-care screening cancer cells was developed.

The importance of G-quadruplexes is associated not only with the protection of the ends of chromosomes for human telomeres, but also in the regulation of gene expression for several gene promoters. Carbazole derivatives have a G-quadruplex stabilizing activity of G-rich regions within the promoter sequences of c-myc, VEGF, c-kit, BCL2, and KRAS proto-oncogenes. Carbazole derivatives are able to discriminate different conformations of nucleic acids. Some of them have high sensitivity and binding preference to quadruplex over duplex structures, while others the opposite. They non-covalently interact with double stranded DNA, the object of testing the activity of new drugs and compounds of potential biological properties, through intercalation and the minor groove binding. Carbazole ligands show duality of interaction – they can bind to the minor groove of AT sites and intercalates at GC sites. These derivatives of structures typical of intercalating compounds (flat chromophore) bind to the minor groove of DNA rich in AT sequences forming more stable and energetically favorable ligand-minor groove complex than those formed by intercalation.

Carbazole derivatives are a promising class of agents against various disorders, potentially useful in clinical studies. However more studies must be executed before carbazole derivatives can be applied into a drug for the potential treatment of various microbial or neurological disorders and carcinomas.

Acknowledgments

The author thanks the Foundation for Polish Science for co-financial support of this study (project "Synthesis of new carbazole ligands, potential inhibitors of telomerase in antitumor therapy") within the PARENT-BRIDGE programme (grant number POMOST-2011-3/3). The author thanks Professor Bernard Juskowiak for reading of the manuscript and student Anna Kowal for the preparation the parts of drawings.

References

[1] K.R.J. Thomas, J.T. Lin, Y.-T. Tao, C.-W. Ko, J. Am. Chem. Soc. 123 (2001) 9404–9411.
[2] A. Van Dijken, J.J.A.M. Bastiaansen, N.M.M. Kiggen, B.M.W. Langeveld, C. Rothe, A. Monkman, I. Bach, P. Stössel, K. Brunner, J. Am. Chem. Soc. 126 (2004) 7718–7727.
[3] H.-y. Fu, H.-r. Wu, X.-y. Hou, F. Xiao, B.-x. Shao, Synth. Met. 156 (2006) 809–814.
[4] A. Ryan, B. Tuffy, S. Horn, W.J. Blau, M.O. Senge, Tetrahedron 67 (2011) 8248–8254.
[5] S.-W. Hwang, Y. Chen, Macromolecules 34 (2001) 2981–2986.
[6] J.-F. Morin, M. Leclerc, D. Adès, A. Siove, Macromol. Rapid Commun. 26 (2005) 761–778.
[7] J.E. McGrath, L. Rasmussen, A.R. Shultz, H.K. Shobha, M. Sankarapandian, T. Glass, T.E. Long, A.J. Pasquale, Polymer 47 (2006) 4042–4057.
[8] J. Qu, R. Morita, H. Ashitaka, N. Ogata, T. Masuda, Polymer 49 (2008) 3663–3670.
[9] N.A. Rice, A. Adronov, Macromolecules 46 (2013) 3850–3860.
[10] D. Kim, J.K. Lee, S.O. Kang, J. Ko, Tetrahedron 63 (2007) 1913–1922.
[11] C. Won Lee, J.Y. Lee, Dyes Pigments 103 (2014) 34–38.
[12] H.-J. Knölker, K.R. Reddy, Chem. Rev. 102 (2002) 4303–4427.
[13] M.E. Peek, L.A. Lipscomb, J.A. Bertrand, Q. Gao, B.P. Roques, C. Garbay-Jaureguiberry, L.D. Williams, Biochemistry 33 (1994) 3794–3800.
[14] J. Ren, C. Bailly, J.B. Chaires, FEBS Lett. 470 (2000) 355–359.
[15] P.B. Arimondo, P. Moreau, A. Boutorine, C. Bailly, M. Prudhomme, J.-S. Sun, T. Garestier, C. Hélène, Bioorg. Med. Chem. 8 (2000) 777–784.
[16] C. Bailly, Curr. Med. Chem. 7 (2000) 39–58.
[17] J. Benoît, M. Facompré, H. Da Costa, S. Routier, J.-Y. Mérour, P. Colson, C. Houssier, C. Bailly, Bioorg. Med. Chem. 9 (2001) 1533–1541.
[18] T. O'Brien, J. Schneider, D. Warshawsky, K. Mitchell, Toxicol. Vitro 16 (2002) 235–243.
[19] C. Asche, W. Frank, A. Albert, U. Kucklaender, Bioorg. Med. Chem. 13 (2005) 819–837.
[20] N. Haider, Curr. Org. Chem. 10 (2006) 363–375.
[21] T. Lemster, U. Pindur, G. Lenglet, S. Depauw, C. Dassi, M.-H. David-Cordonnier, Eur. J. Med. Chem. 44 (2009) 3235–3252.
[22] M.G. Ferlin, C. Marzano, V. Gandin, S. Dall'Acqua, L.D. Via, ChemMedChem 4 (2009) 363–377.
[23] C. Ito, M. Itoigawa, K. Aizawa, K. Yoshida, N. Ruangrungsi, H. Furukawa, J. Nat. Prod. 72 (2009) 1202–1204.
[24] A.C. Adebajo, E.O. Iwalewa, E.M. Obuotor, G.F. Ibikunle, N.O. Omisore, C.O. Adewunmi, O.O. Obaparusi, M. Klaes, G.E. Adetogun, T.J. Schmidt, E.J. Verspohl, J. Ethnopharmacol. 122 (2009) 10–19.
[25] U. Songsiang, T. Thongthoom, C. Boonyarat, C. Yenjai, J. Nat. Prod. 74 (2011) 208–212.
[26] Q. Ma, J. Tian, J. Yang, A. Wang, T. Ji, Y. Wang, Y. Su, Fitoterapia 87 (2013) 1–6.
[27] J. Wang, Y. Zheng, T. Efferth, R. Wang, Y. Shen, X. Hao, Phytochemistry 66 (2005) 697–701.
[28] A. Chakraborty, C. Saha, G. Podder, B.K. Chowdhury, P. Bhattacharyya, Phytochemistry 38 (1995) 787–789.
[29] T.S. Wu, S.C. Huang, P.L. Wu, C.S. Kuoh, Phytochemistry 52 (1999) 523–527.
[30] B. Kongkathip, N. Kongkathip, A. Sunthitikawinsakul, C. Napaswat, C. Yoosook, Phytother. Res. 19 (2005) 728–731.
[31] T. Nakamura, N. Kodama, Y. Arai, T. Kumamoto, Y. Higuchi, C. Chaichantipyuth, T. Ishikawa, K. Ueno, S. Yano, J. Nat. Med. 63 (2009) 21–27.
[32] T. Thongthoom, U. Songsiang, C. Phaosiri, C. Yenjai, Arch. Pharm. Res. 33 (2010) 675–680.
[33] P. Rajakumar, K. Sekar, V. Shanmugaiah, N. Mathivanan, Eur. J. Med. Chem. 44 (2009) 3040–3045.
[34] F.-F. Zhang, L.-L. Gan, C.-H. Zhou, Bioorg. Med. Chem. Lett. 20 (2010) 1881–1884.
[35] M. Saravanabhavan, K. Sathya, V.G. Puranik, M. Sekar, Spectrochim. Acta A Mol. Biomol. Spectrosc. 118 (2014) 399–406.
[36] H.-Y. Lee, Y. Jung, W. Kim, J.H. Kim, M.-S. Suh, S.K. Shin, H.-J. Yoon, Bioorg. Med. Chem. Lett. 18 (2008) 4670–4674.
[37] J. Molette, J. Routier, N. Abla, D. Besson, A. Bombrun, R. Brun, H. Burt, K. Georgi, M. Kaiser, S. Nwaka, M. Muzerelle, A. Scheer, ACS Med. Chem. Lett. 4 (2013) 1037–1041.
[38] B.P. Bandgar, L.K. Adsul, H.V. Chavan, S.S. Jalde, S.N. Shringare, R. Shaikh, R.J. Meshram, R.N. Gacche, V. Masand, Bioorg. Med. Chem. Lett. 22 (2012) 5839–5844.
[39] A. Zall, D. Kieser, N. Höttecke, E.C. Naumann, B. Thomaszewski, K. Schneider, D.T. Steinbacher, R. Schubenel, S. Masur, K. Baumann, B. Schmidt, Bioorg. Med. Chem. 19 (2011) 4903–4909.
[40] W. Yang, Y. Wong, O.T.W. Ng, L.-P. Bai, D.W.J. Kwong, Y. Ke, Z.-H. Jiang, H.-W. Li, K.K.L. Yung, M.S. Wong, Angew. Chem. Int. Ed. 51 (2012) 1804–1810.
[41] C. Saengkhae, M. Salerno, D. Adès, A. Siove, L. Le Moyec, V. Migonney, A. Garnier-Suillerot, Eur. J. Pharmacol. 559 (2007) 124–131.
[42] S. Thiratmatrakul, C. Yenjai, P. Waiwut, O. Vajragupta, P. Reubroycharoen, M. Tohda, C. Boonyarat, Eur. J. Med. Chem. 75 (2014) 21–30.
[43] A.A. Pieper, S. Xie, E. Capota, S.J. Estill, J. Zhong, J.M. Long, G.L. Becker, P. Huntington, S.E. Goldman, C.-H. Shen, M. Capota, J.K. Britt, T. Kotti, K. Ure, D.J. Brat, N.S. Williams, K.S. MacMillan, J. Naidoo, L. Melito, J. Hsieh, J. De Brabander, J.M. Ready, S.L. McKnight, Cell 142 (2010) 39–51.
[44] K.S. MacMillan, J. Naidoo, J. Liang, L. Melito, N.S. Williams, L. Morlock, P.J. Huntington, S.J. Estill, J. Longgood, G.L. Becker, S.L. McKnight, A.A. Pieper, J.K. De Brabander, J.M. Ready, J. Am. Chem. Soc. 133 (2011) 1428–1437.
[45] H.J. Yoon, S.-Y. Kong, M.-H. Park, Y. Cho, S.-E. Kim, J.-Y. Shin, S. Jung, J. Lee, C. Farhanullah, H.-J. Kim, J. Lee, Bioorg. Med. Chem. Lett. 21 (2013) 7165–7174.
[46] I. Arrieta-Cruz, J. Wang, C. Pavlides, G.M. Pasinetti, J. Alzheimers Dis. 21 (2010) 649–654.
[47] J. Wang, K. Ono, D.L. Dickstein, I. Arrieta-Cruz, W. Zhao, X. Qian, A. Lamparello, R. Subnani, M. Ferruzzi, C. Pavlides, L. Ho, P.R. Hof, D.B. Teplow, G.M. Pasinetti, Neurobiol. Aging 32 (2011) 2321.e1–2321.e12.
[48] I. Tasset, C. Espínola, F.J. Medina, M. Feijóo, C. Ruiz, E. Moreno, M.M. Gómez, J.A. Collado, C. Muñoz, J. Muntané, P. Montilla, I. Túnez, J. Physiol. Biochem.

65 (2009) 291–296.
[49] Y. Ouyang, Z. Chen, M. Tan, A. Liu, M. Chen, J. Liu, R. Pi, J. Fang, Biochem. Biophys. Res. Commun. 441 (2013) 917–922.
[50] A. Kumar, A. Prakash, S. Dogra, Pharmacol. Rep. 63 (2011) 915–923.
[51] D. Zhu, M. Chen, M. Li, B. Luo, Y. Zhao, P. Huang, F. Xue, S. Rapposelli, R. Pi, S. Wen, Eur. J. Med. Chem. 68 (2013) 81–88.
[52] L.-C. Chang, L.-T. Tsao, C.-S. Chang, C.-J. Chen, L.-J. Huang, S.-C. Kuo, R.-H. Lin, J.-P. Wang, Biochem. Pharmacol. 76 (2008) 507–519.
[53] M.-J. Hsu, Y. Chao, Y.-H. Chang, F.-M. Ho, L.-J. Huang, Y.-L. Huang, T.-Y. Luh, C.-P. Chen, W.-W. Lin, Biochem. Pharmacol. 70 (2005) 102–112.
[54] L. Hu, Z.-r. Li, Y. Li, J. Qu, Y.-H. Ling, J.-d. Jiang, D.W. Boykin, J. Med. Chem. 49 (2006) 6273–6282.
[55] L. Nagarapu, H.K. Gaikwad, K. Sarikonda, J. Mateti, R. Bantu, P.S. Raghu, K.M. Manda, S.V. Kalvendi, Eur. J. Med. Chem. 45 (2010) 4720–4725.
[56] S. Yoon, J.-H. Kim, Y.J. Lee, M.Y. Ahn, G. Choi, W.K. Kim, Z. Yang, H.J. Lee, H.R. Moon, H.S. Kim, Eur. J. Pharmacol. 697 (2012) 24–31.
[57] A. Caruso, M.S. Sinicropi, J.-C. Lancelot, H. El-Kashef, C. Saturnino, G. Aubert, C. Ballandonne, A. Lesnard, T. Cresteil, P. Dallemagne, S. Rault, Bioorg. Med. Chem. Lett. 24 (2014) 467–472.
[58] C. Asche, M. Demeunynck, Anticancer Agents Med. Chem. 7 (2007) 247–267.
[59] C.-C. Chang, J.-Y. Wu, T.-C. Chang, J. Chin. Chem. Soc. 50 (2003) 185–188.
[60] C.-C. Chang, I.-C. Kuo, J.-J. Lin, Y.-C. Lu, C.-T. Chen, H.-T. Back, P.-J. Lou, T.-Ch Chang, Chem. Biodivers. 1 (2004) 1377–1384.
[61] F.-C. Huang, C.-C. Chang, P.-J. Lou, I.-C. Kuo, C.-W. Chien, C.-T. Chen, F.-Y. Shieh, T.-C. Chang, J.-J. Lin, Mol. Cancer Res. 6 (2008) 955–964.
[62] C.-C. Kang, W.-C. Huang, C.-W. Kouh, Z.-F. Wang, C.-C. Cho, C.-C. Chang, C.-L. Wang, T.-C. Chang, J. Seemannf, L.J.-s. Huang, Integr. Biol. 5 (2013) 1217–1228.
[63] F.-C. Huang, C.-C. Chang, J.-M. Wang, T.-C. Chang, J.-J. Lin, Br. J. Pharmacol. 167 (2012) 393–406.
[64] J.F. Chu, Z.F. Wang, T.Y. Tseng, T.C. Chang, J. Chin. Chem. Soc. 58 (2011) 296–300.
[65] T.-Y. Tseng, C.-H. Chien, J.-F. Chu, W.-C. Huang, M.-Y. Lin, C.-C. Chang, T.-C. Chang, J. Biomed. Opt. 18 (2013) 101309.
[66] Y.-S. Chou, C.-C. Chang, T.-C. Chang, T.-L. Yang, T.-H. Young, P.-J. Lou, BioMed. Res. Int. (2013) 10.
[67] T.-Y. Tseng, Z.-F. Wang, C.-H. Chien, T.-C. Chang, Nucleic Acids Res. 41 (2013) 10605–10618.
[68] C.-C. Kang, C.-C. Chang, T.-C. Chang, L.-J. Liao, P.-J. Lou, W. Xie, E.S. Yeung, Analyst 132 (2007) 745–749.
[69] L.-J. Liao, C.-C. Kang, I.-S. Jan, H.-C. Chen, C.-L. Wang, P.-J. Lou, T.-C. Chang, Analyst 134 (2009) 708–711.
[70] T.-L. Yang, L. Lin, P.-J. Lou, T.-C. Chang, T.-H. Young, PLoS One 9 (2014) e86143.
[71] I.-T. Lin, Y.-L. Tsai, C.-C. Kang, W.-C. Huang, C.-L. Wang, M.-Y. Lin, P.-J. Lou, J.-Y. Shih, H.-C. Wang, H.-D. Wu, T.-H. Tsai, I.-S. Jan, T.-C. Chang, Cancer Med. 3 (2014) 162–173.
[72] J.-M. Wang, F.-C. Huang, M. Hsin-Jui Kuo, Z.-F. Wang, T.-Y. Tseng, L.-C. Chang, S.-J. Yen, T.-C. Chang, J.-J. Lin, J. Biol. Chem. 289 (2014) 14612–14623.
[73] N. Dias, U. Jacquemard, B. Baldeyrou, C. Tardy, A. Lansiaux, P. Colson, F. Tanious, W.D. Wilson, S. Routier, J.-Y. Mérour, C. Bailly, Biochemistry 43 (2004) 15169–15178.
[74] J. Li, D. Li, Y. Han, S. Shuang, C. Dong, Spectrochim. Acta Part A 73 (2009) 221–225.
[75] B. Dumat, G. Bordeau, E. Faurel-Paul, F. Mahuteau-Betzer, N. Saettel, M. Bombled, G. Metgé, F. Charra, C. Fiorini-Debuisschert, M.-P. Teulade-Fichou, Biochimie 93 (2011) 1209–1218.
[76] A. Głuszyńska, K. Bajor, I. Czerwińska, D. Kalet, B. Juskowiak, Tetrahedron Lett. 51 (2010) 5415–5418.
[77] A. Głuszyńska, E. Rajczak, B. Juskowiak, in: Proceedings of the 39th International Conference of Slovak Society of Chemical Engineering, 2012, pp. 1349–1354.
[78] A. Głuszyńska, E. Rajczak, B. Juskowiak, Chem. Pap. 67 (2013) 1231–1239.
[79] A. Głuszyńska, E. Rajczak, J. Kosman, B. Juskowiak, in: Proceedings of the 40th International Conference of Slovak Society of Chemical Engineering, 2013, pp. 1326–1332.
[80] A. Głuszyńska, K. Burzyńska, E. Rajczak, B. Juskowiak, in: Proceedings of the 41th International Conference of Slovak Society of Chemical Engineering, 2014, pp. 526–530.
[81] Unpublished results.
[82] C.-C. Chang, J.-Y. Wu, C.-W. Chien, W.-S. Wu, H. Liu, C.-C. Kang, L.-J. Yu, T.-C. Chang, Anal. Chem. 75 (2003) 6177–6183.
[83] C.-C. Chang, I.-C. Kuo, I.-F. Ling, C.-T. Chen, H.-C. Chen, P.-J. Lou, J.-J. Lin, T.-C. Chang, Anal. Chem. 76 (2004) 4490–4494.
[84] C.-C. Chang, J.-F. Chu, F.-J. Kao, Y.-C. Chiu, P.-J. Lou, H.-C. Chen, T.-C. Chang, Anal. Chem. 78 (2006) 2810–2815.
[85] C.-C. Chang, C.-W. Chien, Y.-H. Lin, C.-C. Kang, T.-C. Chang, Nucleic Acids Res. 35 (2007) 2846–2860.
[86] D.-Y. Yang, T.-C. Chang, S.-Y. Sheu, J. Phys. Chem. A 111 (2007) 9224–9232.
[87] T.-C. Chang, C.-C. Chang, in: P. Baumann (Ed.), G-Quadruplex DNA: Methods and Protocols, Methods in Molecular Biology, vol. 608, Humana Press, 2010, pp. 183–206.
[88] X.-f. Zhang, H.-j. Zhang, J.-f. Xiang, Q. Li, Q.-f. Yang, Q. Shang, Y.-x. Zhang, Y.-l. Tang, J. Mol. Biol. 982 (2010) 133–138.
[89] X.J. Feng, P.Z. Tian, Z. Xu, S.F. Chen, M.S. Wong, J. Org. Chem. 78 (2013) 11318–11325.
[90] M. Gellert, M.N. Lipsett, R.D. Davies, Proc. Natl. Acad. Sci. U. S. A. 48 (1962) 2013–2016.
[91] D. Sun, B. Thompson, B.E. Cathers, M. Salazar, S.M. Kerwin, J.O. Trent, T.C. Jenkins, S. Neidle, L.H. Hurley, J. Med. Chem. 40 (1997) 2113–2116.
[92] J.-F. Riou, Curr. Med. Chem. Anti-Cancer Agents 4 (2004) 439–443.
[93] L.R. Kelland, Eur. J. Cancer 41 (2005) 971–979.
[94] A. De Cian, L. Lacroix, C. Douarre, N. Temime-Smaali, C. Trentesaux, J.-F. Riou, J.-L. Mergny, Biochemie 90 (2008) 131–155.
[95] T. Ou, Y. Lu, J. Tan, Z. Huang, K. Wong, L. Gu, ChemMedChem 3 (2008) 690–713.
[96] M. Folini, P. Gandellini, N. Zaffaroni, Biochim. Biophys. Acta 1792 (2009) 309–316.
[97] T.A. Brooks, L.H. Hurley, Genes Cancer 1 (2010) 641–649.
[98] C. Bruhlmann, F. Ooms, P.A. Carrupt, B. Testa, M. Catto, F. Leonetti, C. Altomare, A. Carotti, J. Med. Chem. 44 (2001) 3195–3198.
[99] M.B. Youdim, T. Amit, M. Falach-Yogev, O. Bar Am, W. Maruyama, M. Naoi, Biochem. Pharmacol. 66 (2003) 1635–1641.
[100] G. Perry, A.D. Cash, M.A. Smith, J. Biomed. Biotechnol. 2 (2002) 120–123.
[101] V. Tumiatti, A. Minarini, M.L. Bolognesi, A. Milelli, M. Rosini, C. Melchiorre, Curr. Med. Chem. 17 (2010) 1825–1838.
[102] J. Altman, Science 135 (1962) 1127–1128.
[103] J. Altman, G.D. Das, J. Comp. Neurol. 124 (1965) 319–335.
[104] C.G. Gross, Natl. Rev. 1 (2000) 67–72.
[105] K.L. Spalding, O. Bergmann, K. Alkass, S. Bernard, M. Salehpour, H.B. Huttner, E. Boström, I. Westerlund, C. Vial, B.A. Buchholz, G. Possnert, D.C. Mash, H. Druid, J. Frisén, Cell 153 (2013) 1219–1227.
[106] P. Dandona, H. Ghanim, D.P. Brooks, J. Hypertens. 25 (2007) 731–741.
[107] T. Hayashi, Y. Saitou, K. Nose, T. Nishioka, T. Ishii, H. Uemura, Transpl. Proc. 40 (2008) 2139–2141.
[108] P.B. Rosenberg, M.M. Mielke, J. Tschanz, L. Cook, C. Corcoran, K.M. Hayden, M. Norton, P.V. Rabins, R.C. Green, K.A. Welsh-Bohmer, J.C. Breitner, R. Munger, C.G. Lyketsos, Am. J. Geriatr. Psychiatry 16 (2008) 883–892.
[109] J. Wang, L. Ho, L. Chen, Z. Zhao, W. Zhao, X. Qian, N. Humala, I. Seror, S. Bartholomew, C. Rosendorff, G.M. Pasinetti, J. Clin. Invest. 117 (2007) 3393–3402.
[110] S.I. Savitz, J.A. Erhardt, J.V. Anthony, G. Gupta, X. Li, F.C. Barone, D.M. Rosenbaum, J. Cereb. Blood Flow. Metab. 20 (2000) 1197–1204.
[111] R.M. Abreu, D.J. Santos, A.J. Moreno, J. Pharmacol. Exp. Ther. 295 (2000) 1022–1030.
[112] P.G. Lysko, K.A. Lysko, T.L. Yue, C.L. Webb, J.L. Gu, G. Feuerstein, Stroke 23 (1992) 1630–1635.
[113] B. Macedo, J. Magalhães, A.R. Batista, M.J. Saraiva, Pharmacol. Res. 62 (2010) 514–522.
[114] T. Yoshioka, N. Iwamoto, F. Tsukahara, K. Irie, I. Urakawa, T. Muraki, Br. J. Pharmacol. 129 (2000) 1530–1535.
[115] K. Oettl, J. Greilberger, K. Zangger, E. Haslinger, G. Reibnegger, G. Jürgens, Biochem. Pharmacol. 62 (2001) 241–248.
[116] I. Tunez, J.A. Collado, F.J. Medina, M.C. Munoz, R. Gordillo, C. Sampedro, M.J. Moyano, M. Feijoo, J. Muntane, P. Montilla, Pharmacol. Res. 54 (2006) 241–246.
[117] D.R. Howlett, A.R. George, D.E. Owen, R.V. Ward, R.E. Markwell, Biochem. J. 343 (1999) 419–423.
[118] J. Bart, E.C. Dijkers, T.D. Wegman, E.G. de Vries, W.T. van der Graaf, H.J. Groen, W. Vaalburg, A.T. Willemsen, N.H. Hendrikse, Br. J. Pharmacol. 145 (2005) 1045–1051.
[119] B. Dulin, W.T. Abraham, Am. J. Cardiol. 6 (2004) 3–6.
[120] M.J. Calkins, D.A. Johnson, J.A. Townsend, M.R. Vargas, J.A. Dowell, T.P. Williamson, A.D. Kraft, J.M. Lee, J. Li, J.A. Johnson, Antioxid. Redox Signal. 11 (2009) 497–508.
[121] A. Scozzafava, T. Owa, A. Mastrolorenzo, C.T. Supuran, Curr. Med. Chem. 10 (2003) 925–953.
[122] A. Casini, A. Scozzafava, A. Mastrolorenzo, C.T. Supuran, Curr. Cancer Drug Targets 2 (2002) 55–75.
[123] N.D. Hastie, M. Dempster, M.G. Dunlop, A.M. Thompson, D.K. Green, R.C. Allshire, Nature 346 (1990) 866–868.
[124] J.W. Shay, S. Bacchetti, Eur. J. Cancer 33 (1997) 787–791.
[125] S.E. Holt, J.W. Shay, J. Cell. Physiol. 180 (1999) 10–18.
[126] R.J. O'Sullivan, J. Karlseder, Nat. Rev. Mol. Cell. Biol. 11 (2010) 171–181.
[127] E.H. Blackburn, Nature 350 (1991) 569–573.
[128] C.M. Counter, A.A. Avilion, C.E. LeFeuvre, N.G. Stewart, C.W. Greider, C.B. Harley, S. Bacchettil, EMBO J. 11 (1992) 1921–1929.
[129] A. Siddiqui-Jain, C.L. Grand, D.J. Bearss, L.H. Hurley, Proc. Natl. Acad. Sci. U. S. A. 99 (2002) 11593–11598.
[130] H.J. Lipps, D. Rhodes, Trends Cell. Biol. 19 (2009) 414–422.
[131] G. Biffi, D. Tannahill, J. McCafferty, S. Balasubramanian, Nat. Chem. 5 (2013) 182–186.
[132] A.K. Todd, M. Johnston, S. Neidle, Nucleic Acids Res. 33 (2005) 2901–2907.
[133] J.L. Huppert, S. Balasubramanian, Nucleic Acids Res. 33 (2005) 2908–2916.
[134] A. Siddiqui-Jain, C.L. Grand, D.J. Bearss, L.H. Hurley, Proc. Natl. Acad. Sci. U. S. A. 99 (2004) 11593–11598.
[135] S. Rankin, A.P. Reszka, J. Huppert, M. Zloh, G.N. Parkinson, A.K. Todd, S. Ladame, S. Balasubramanian, S. Neidle, J. Am. Chem. Soc. 127 (2005) 10584–10589.
[136] D. Sun, K. Guo, J.J. Rusche, L.H. Hurley, Nucleic Acids Res. 33 (2005)

6070–6080.
[137] J. Dai, T.S. Dexheimer, D. Chen, M. Carver, A. Ambrus, R.A. Jones, D. Yang, J. Am. Chem. Soc. 128 (2006) 1096–1098.
[138] S. Cogoi, L.E. Xodo, Nucleic Acids Res. 34 (2006) 2536–2549.
[139] J. Cuesta, M.A. Read, S. Neidle, Mini Rev. Med. Chem. 3 (2003) 11–21.
[140] Y. Pommier, Biochimie 80 (1998) 255–270.
[141] L.R. Kelland, Anti-Cancer Drugs 11 (2000) 503–513.
[142] J. Perry, T.C. Jenkins, Mini Rev. Med. Chem. 1 (2001) 31–41.
[143] X. Zhang, V. Mar, W. Zhou, L. Harrington, M.O. Robinson, Genes. Dev. 13 (1999) 2388–2399.
[144] J.W. Shay, W.E. Wright, Cancer Cell. 2 (2002) 257–265.
[145] J.W. Shay, W.E. Wright, Nat. Rev. Drug Discov. 5 (2006) 577–584.
[146] S. Neidle, G. Parkinson, Nat. Rev. Drug Discov. 1 (2002) 383–393.
[147] M.K. Raghuraman, T.R. Cech, Nucleic Acids Res. 18 (1990) 4543–4552.
[148] W.D. Wilson, F.A. Tanious, D. Ding, A. Kumar, D.W. Boykin, P. Colson, C. Houssier, C. Bailly, J. Am. Chem. Soc. 120 (1998) 10310–10321.
[149] P. Colson, C. Houssier, C. Bailly, J. Biomol. Struct. Dyn. 13 (1995) 351–366.
[150] W.D. Wilson, F.A. Tanious, H.J. Barton, L. Strekowski, D.W. Boykin, J. Am. Chem. Soc. 111 (1989) 5008–5010.
[151] W.D. Wilson, F.A. Tanious, H.J. Barton, R.L. Jones, K.R. Fox, R.L. Wydra, L. Strekowski, Biochemistry 29 (1990) 8452–8461.
[152] F.A. Tanious, J. Spychala, A. Kumar, K. Greene, D.W. Boykin, W.D. Wilson, J. Biomol. Struct. Dyn. 11 (1994) 1063–1083.
[153] E. Gałęzowska, A. Masternak, B. Rubiś, A. Czyrski, M. Rybczyńska, T.W. Hermann, B. Juskowiak, Int. J. Biol. Macromol. 41 (2007) 558–563.
[154] B. Rubiś, M. Kaczmarek, N. Szymanowska, E. Gałęzowska, A. Czyrski, B. Juskowiak, T.W. Hermann, M. Rybczyńska, Invest. New. Drugs 27 (2009) 289–296.
[155] I. Czerwińska, B. Juskowiak, Int. J. Biol. Macromol. 51 (2012) 576–582.
[156] J.-Y. Wu, C.-C. Chang, C.-S. Yan, K.-Y. Chen, I.-C. Kuo, C.-Y. Mou, T.-C. Chang, J. Biomol. Struct. Dyn. 21 (2003) 135–140.
[157] P. Hazel, J. Huppert, S. Balasubramanian, S. Neidle, J. Am. Chem. Soc. 126 (2004) 16405–16415.